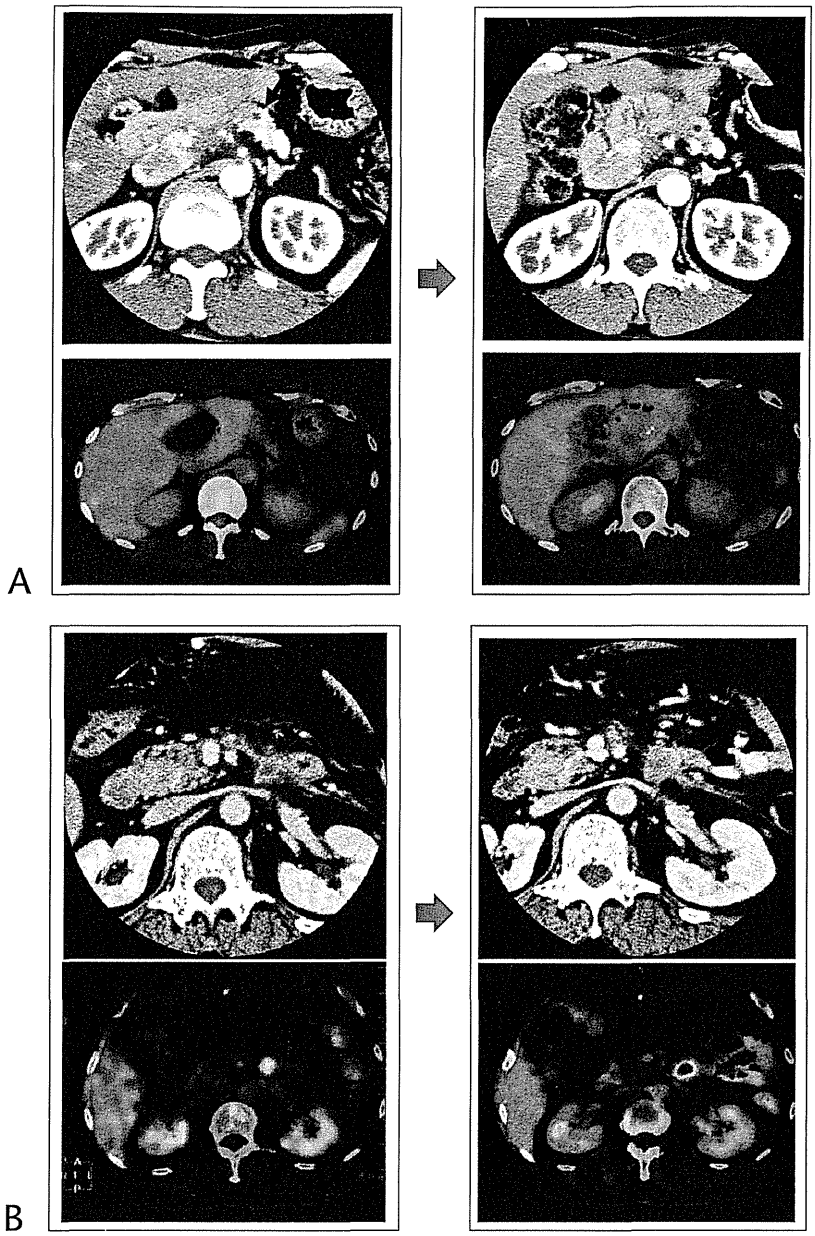

FIGURE 5. Positron emission tomography/CE-CT findings of 2 typical cases, 1 with "local recurrence" and the other with "no local recurrence," are shown. A, A 46-year-old man with no local recurrence (false-positive by CE-CT and true-negative by PET/CE-CT). The CE-CT image, which was performed 17 months after surgery, showed a soft tissue density mass, which did not rule out local recurrence (left upper panel, arrow). However, the PET/CT image did not show FDG uptake corresponding to this mass, suggesting no local recurrence (left lower panel, arrow). A follow-up PET/CE-CT image, which was performed 8 months after the initial examination, revealed no increase in the size and FDG uptake of the mass (right panel, arrow), indicating that the initial diagnosis of no local recurrence by PET/CE-CT was correct. B, A 59-year-old man with local recurrence (true-positive by CE-CT and PET/CE-CT). The CE-CT image, which was performed 3 months after surgery, showed a soft tissue density mass, which did not rule out local recurrence (left upper panel, arrow). The PET/CT image shows abnormal FDG uptake (SUV_{max}, 4.73) corresponding to this mass, suggesting local recurrence (left lower panel, arrow). A follow-up PET/CE-CT image, which was performed 3 months after the initial examination, revealed an increase in the size and FDG uptake (SUV_{max}, 6.99) of the mass (right panel, arrow), indicating that the initial diagnosis of local recurrence by PET/CE-CT was correct.

the N factor, which is consistent with previous reports.[16,17] On the other hand, PET/CE-CT is very useful in evaluation of the M factor, as indicated by the high accuracy rate of PET/CE-CT within this context. In fact, the diagnostic accuracy rate of PET/CE-CT for the M factor was 94% in 31 patients with stage IVa resectable cancers. Furthermore, in 65 patients with stage IVb

unresectable cancers, the detection rates of PET/CE-CT for metastases to the lymph nodes (N3), liver, peritoneum, lung, and bone were 51%, 55%, 53%, 18%, and 24%, respectively. These detection rates for distant lymph node (N3) and peritoneum metastases were significantly higher for PET/CE-CT imaging than for abdominal CE-CT imaging. The detection rates of PET/CE-CT for lung and bone metastases were also higher than those of abdominal CE-CT imaging. However, such differences were attributed to the nature of PET/CE-CT scans (whole body imaging) and abdominal CE-CT scans (imaging of only a segmental area). Therefore, in the preoperative evaluation of the extent of pancreatic cancer, which is important for deciding treatment options, our present results suggest that PET/CE-CT is a useful tool for assessing T and M factors but is not very useful for assessing the N factor. This is consistent with a report by Strobel et al,[18] in which PET/CE-CT was found to be superior to PET imaging alone in assessing the respectability of pancreatic cancer.

When PET was first developed, many published reports stated that the SUV_{max} could be useful for differentially diagnosing malignancies and benignancies.[16,19] Nishiyama et al[20] and Nakamoto et al[21] reported that a malignancy could be differentiated from a benignancy in pancreatic disorders based on the SUV_{max}-to-delayed scan ratio. However, as described in the present study, the SUV_{max} of malignant pancreatic tumors overlapped with that of benign pancreatic diseases, suggesting that distinguishing between benign and malignant cases through SUV_{max}-based diagnosis is difficult. Extremely high SUV_{max} values were observed in 2 cases of benign pancreatic endocrine tumor in the present study. The SUV_{max} varies according to the several factors, including blood glucose levels, Glut 1 expression, glucose-6-phosphatase expression, and tumor heterogeneity, and others.[16] In a previous study, high SUV_{max} values were found in tumors with high Glut 1 expression.[22] In our study, extremely high SUV_{max} values were observed in 2 cases of benign endocrine tumors, and these high values may be attributed to high Glut 1 expression in these tumors; however, Glut 1 expression was not examined histologically. To differentiate between benignancy and malignancy of pancreatic tumor lesions by PET/CE-CT imaging, we first assessed the invasion of the tumors into surrounding organs/vessels and other malignancy—indicating signs by analysis of the CE-CT portion of PET/CE-CT imaging and then diagnosed the case by referring to the FDG uptake data (SUV_{max}) by analysis of the PET portion. We did not use SUV_{max} values for differentiating between benignancy and malignancy. So, what is the meaning of SUV_{max} in the clinical management of pancreatic cancer? In the present study, we examined correlations between the SUV_{max}, Ts, and tumor marker (CA 19-9) levels in unresectable locally advanced pancreatic cancer under treatment. During the course of treatment, SUV_{max} and CA 19-9 levels showed substantial positive correlations in the change rate, whereas SUV_{max} and Ts showed significant, although slight, positive correlations. However, no significant correlation was found between tumor marker levels and Ts. Treatment effects on solid tumors were assessed by determining Ts by imaging according to the RECIST criteria[12] and by the levels of serum tumor markers. In pancreatic cancer, however, changes in Ts do not necessarily reflect treatment effects because pancreatic cancers contain a variety of interstitial components. Thus, we have frequently experienced discrepancies between changes in Ts and tumor marker levels in assessing the effects of treatment, which makes it difficult to determine the effects of treatment in these cases. Identification of an additional indicator would help in determining the effects of treatment on pancreatic cancer progression/regression. In the present study, we demonstrated that the SUV_{max} measured by PET proved useful in this regard. Similarly, Yoshioka et al[23] reported that the SUV_{max} was useful to monitor the effects of treatment on pancreatic cancers. These findings, together with those in the present study, suggest that the SUV_{max} is a useful indicator for the effects of treatment on pancreatic cancer. The addition of the SUV_{max} to the existing indicators (Ts and markers) is expected to reduce the difficulty of assessing the effects of treatment on pancreatic cancer progression.

Because either invasion into the surrounding regions or distant metastasis is often already involved at the time of pancreatic cancer diagnosis, less than 20% of cases are treated surgically.[24] Even when surgery is used, recurrence usually occurs very soon thereafter.[13] Therefore, cautious observation is required after surgery. In general, abdominal CE-CT is conducted every 3 to 6 months for postoperative monitoring. Local, hepatic, and peritoneal recurrences are frequently observed postoperatively. Abdominal CE-CT can be used to diagnose hepatic recurrence, but it is sometimes difficult to detect local or peritoneal recurrences because of postoperative changes in the anatomical positions of organs.[15,17] Ruf et al[25] showed that FDG-PET is superior to CT/magnetic resonance imaging in the detection of local recurrences of pancreatic cancers. In the present study, we demonstrated that the diagnostic accuracy of PET/CE-CT is superior to abdominal CE-CT in predicting the postoperative local recurrence of pancreatic cancer. Considering the postoperative changes in the anatomical positions of abdominal organs, PET/CE-CT imaging, which uses both CE-CT and PET functions, is recommended for postoperative monitoring.

CONCLUSIONS

In the present study, we demonstrated that PET/CE-CT imaging can provide useful information in the clinical management of pancreatic cancer. We recommend PET/CE-CT imaging as the first choice examination for suspected pancreatic cancer, staging, assessment of treatment effectiveness, and confirmation of suspected recurrence.

REFERENCES

1. Jemal A, Siegel R, Xu J, et al. Cancer statistics, 2010. *CA Cancer J Clin*. 2010;60:277–300.
2. Matsuda T, Marugame T, Kamo K, et al. Cancer incidence and incidence rates in Japan in 2003: based on data from 13 population-based cancer registries in the Monitoring of Cancer Incidence in Japan (MCIJ) Project. *Jpn J Clin Oncol*. 2009;39:850–858.
3. Burris HA 3rd, Moore MJ, Andersen J, et al. Improvements in survival and clinical benefit with gemcitabine as first-line therapy for patients with advanced pancreas cancer: a randomized trial. *J Clin Oncol*. 1997;15:2403–2413.
4. Okusaka T, Funakoshi A, Furuse J, et al. A late phase II study of S-1 for metastatic pancreatic cancer. *Cancer Chemother Pharmacol*. 2008;61:615–621.
5. Smith SL, Rajan PS. Imaging of pancreatic adenocarcinoma with emphasis on multidetector CT. *Clin Radiol*. 2004;59:26–38.
6. Ell PJ. The contribution of PET/CT to improved patient management. *Br J Radiol*. 2006;79:32–36.
7. Reinartz P, Wieres FJ, Schneider W, et al. Side-by-side reading of PET and CT scans in oncology: which patients might profit from integrated PET/CT? *Eur J Nucl Med Mol Imaging*. 2004;31:1456–1461.
8. Isaji S, Kawarada Y, Uemoto S. Classification of pancreatic cancer: comparison of Japanese and UICC classifications. *Pancreas*. 2004;28:231–234.
9. Otsuki M. Chronic pancreatitis in Japan: epidemiology, prognosis, diagnostic criteria, and future problems. *J Gastroenterol*. 2003;38:315–326.

10. Okazaki K, Kawa S, Kamisawa T, et al. Clinical diagnostic criteria of autoimmune pancreatitis: revised proposal. *J Gastroenterol.* 2006;41:626–631.
11. DeLellis R, Lloyd R, Heitz P, et al, eds. *Pathology and Genetics Tumor of Endocrine Organs (World Health Organization Classification of Tumors).* Lyon, France: IARC Press; 2004.
12. Therasse P, Arbuck SG, Eisenhauer EA, et al. New guidelines to evaluate the response to treatment in solid tumors. European Organization for Research and Treatment of Cancer, National Cancer Institute of the United States, National Cancer Institute of Canada. *J Natl Cancer Inst.* 2000;92:205–216.
13. Geer RJ, Brennan MF. Prognostic indicators for survival after resection of pancreatic adenocarcinoma. *Am J Surg.* 1993;165:68–72.
14. Goldberg RM, Fleming TR, Tangen CM, et al. Surgery for recurrent colon cancer: strategies for identifying resectable recurrence and success rates after resection. Eastern Cooperative Oncology Group, the North Central Cancer Treatment Group, and the Southwest Oncology Group. *Ann Intern Med.* 1998;129:27–35.
15. Barkin JS, Goldstein JA. Diagnostic approach to pancreatic cancer. *Gastroenterol Clin North Am.* 1999;28:709–722.
16. Higashi T, Saga T, Nakamoto Y, et al. Diagnosis of pancreatic cancer using fluorine-18 fluorodeoxyglucose positron emission tomography (FDG PET)—usefulness and limitations in "clinical reality." *Ann Nucl Med.* 2003;17:261–279.
17. Zimny M, Bares R, Fass J, et al. Fluorine-18 fluorodeoxyglucose positron emission tomography in the differential diagnosis of pancreatic carcinoma: a report of 106 cases. *Eur J Nucl Med.* 1997;24:678–682.
18. Strobel K, Heinrich S, Bhure U, et al. Contrast-enhanced ^{18}F-FDG PET/CT: 1-stop-shop imaging for assessing the resectability of pancreatic cancer. *J Nucl Med.* 2008;49:1408–1413.
19. Delbeke D, Rose DM, Chapman WC, et al. Optimal interpretation of FDG PET in the diagnosis, staging and management of pancreatic carcinoma. *J Nucl Med.* 1999;40:1784–1791.
20. Nishiyama Y, Yamamoto Y, Monden T, et al. Evaluation of delayed additional FDG PET imaging in patients with pancreatic tumour. *Nucl Med Commun.* 2005;26:895–901.
21. Nakamoto Y, Higashi T, Sakahara H, et al. Delayed (18)F-fluoro-2-deoxy-D-glucose positron emission tomography scan for differentiation between malignant and benign lesions in the pancreas. *Cancer.* 2000;89:2547–2554.
22. Higashi T, Tamaki N, Honda T, et al. Expression of glucose transporters in human pancreatic tumors compared with increased FDG accumulation in PET study. *J Nucl Med.* 1997;38:1337–1344.
23. Yoshioka M, Sato T, Furuya T, et al. Role of positron emission tomography with 2-deoxy-2-[^{18}F]fluoro-D-glucose in evaluating the effects of arterial infusion chemotherapy and radiotherapy on pancreatic cancer. *J Gastroenterol.* 2004;39:50–55.
24. Wray CJ, Ahmad SA, Matthews JB, et al. Surgery for pancreatic cancer: recent controversies and current practice. *Gastroenterology.* 2005;128: 1626–1641.
25. Ruf J, Lopez Hanninen E, Oettle H, et al. Detection of recurrent pancreatic cancer: comparison of FDG-PET with CT/MRI. *Pancreatology.* 2005;5:266–272.

The bisphosphonate incadronate inhibits intraperitoneal dissemination in an *in vivo* pancreatic cancer model

SOICHI TAKIGUCHI[1], YUKIKO NISHINO[1], KAZUKO INOUE[1], MIYAKO IKEDA[3], YASUFUMI KATAOKA[3], KIMIHIKO MATSUSUE[4], KENICHI NISHIYAMA[2] and HARUO IGUCHI[5]

[1]Institute for Clinical Research and [2]Department of Pathology, National Kyushu Cancer Center, Fukuoka 811-1395; Departments of [3]Pharmaceutical Care and Health Sciences and [4]Hygiene Chemistry, Faculty of Pharmaceutical Sciences, Fukuoka University, Fukuoka 814-0180; [5]Clinical Research Institute, Shikoku Cancer Center, Matsuyama 791-0280, Japan

Received January 17, 2012; Accepted March 14, 2012

DOI: 10.3892/or.2012.1757

Abstract. Pancreatic cancer is characterized by intraperitoneal dissemination and often by large volumes of ascites. Aminobisphosphonates exhibit potent antitumor effects and are currently being tested against human solid tumors. Several aminobisphosphonates inhibit cancer cell migration by preventing the activation of Rho through inhibition of the mevalonate pathway. We evaluated the ability of an aminobisphosphonate, incadronate, to inhibit the growth of disseminated pancreatic cancer *in vivo*. We established an *in vivo* pancreatic cancer model with i.p. carcinomatosis in nude mice. Incadronate administration started from the day of tumor inoculation, and reduced tumor burden and ascites accumulation. Further, we evaluated the effect of incadronate on the inhibition of pancreatic cancer cell proliferation, migration and invasion *in vitro*. Incadronate induced growth inhibition and apoptotic death of pancreatic cancer cells. It also inhibited migration presumably by preventing the activation of Rho by lysophosphatidic acid. Thus, the *in vivo* antitumor effect may result from the inhibition of cancer cell proliferation and migration. The potent effects of incadronate in reducing tumor burden and ascites suggest that it will be of value in regimens for the treatment of pancreatic cancer.

Introduction

Pancreatic cancer is the fourth most common cause of cancer death in men and women in the United States, with a 5-year survival for all stages of the disease of less than 5% (1). Pancreatic cancer has no clear early warning signs or symptoms and is usually silent until the disease is well advanced. During the progression of pancreatic cancer, hepatic metastasis and peritoneal dissemination are frequently seen as a distant metastasis, which results in a short survival period. Patients have a median survival of 4-8 months after diagnosis due to the advanced stage of disease by the time it has been discovered and treatment has begun. The anti-metabolite agent gemcitabine is currently being employed to treat pancreatic cancer (2). While gemcitabine has shown a significant benefit in clinical applications, its ability to impact pancreatic cancer is limited. Therefore, new therapeutic approaches need to be investigated to improve the treatment of this neoplasm (3).

One new therapeutic strategy is to clarify the mechanism of metastasis of cancer cells and to identify agents that prevent cancer cells from invading or migrating into the peritoneum. Among many growth-promoting factors known to be present in pancreatic cancer ascites, lysophosphatidic acid (LPA) is found in significant levels and may play an important role in the development or progression of ovarian (4,5) and pancreatic cancer (6). LPA has been reported to induce many cellular effects, including mitogenesis, the secretion of proteolytic enzymes, and migration activity (7).

Cell migration is regulated by a combination of different processes: the contraction of actomyosin, the formation of stress fibers, and the turnover of focal adhesions (8). Contraction of the actomyosin system is important for cell migration, and LPA induces myosin light-chain phosphorylation through the activation of the small GTP-binding protein (G protein) Rho, leading to the stimulation of cell contractility and motility (9). Another fundamental component affecting cell motility is focal adhesions (cell-extracellular matrix adhesions) (8). Rho is a key mediator in the assembly of structures involved in focal adhesion. Changes in the expression and activities of the components of focal adhesions may contribute to cancer invasion (10). Interfering with the LPA signal transduction pathway by modulating Rho activity may be an attractive strategy for improving the outcome of pancreatic cancer.

Aminobisphosphonates (N-BPs) are potent inhibitors of bone resorption used for the treatment and prevention of osteoporosis. N-BPs have been shown to inhibit the cholesterol biosynthesis pathway as well as isoprenylation (farnesylation and geranylgeranylation) by inhibiting either isopentanyl diphosphate synthase or a downstream enzyme, farnesyl diphosphate synthase, or both (11). Protein targets of isoprenylation include small G proteins

Correspondence to: Dr Haruo Iguchi, Clinical Research Institute, Shikoku Cancer Center, Minamiumemotomachi Ko160, Matsuyama, Ehime 791-0280, Japan
E-mail: higuchi@shikoku-cc.go.jp

Key words: bisphosphonate, apoptosis, pancreatic cancer, intraperitoneal dissemination, Rho

such as Rho, Ras, Rac, and Rab, which require post-translational modification to undergo a series of changes that lead to their attachment to the plasma membrane and their full activation. The activation of small G proteins is essential for cancer cell growth and invasion (12,13). Accordingly, N-BPs have the potential to inactivate the small G proteins that regulate cancer cell growth, motility, and invasion (14,15). Treatment of ovarian cancer cells with alendronate, an N-BP, resulted in the inactivation of Rho, changes in cell morphology, loss of stress fiber formation, and focal adhesion assembly (16). Furthermore alendronate markedly inhibited the invasiveness of human ovarian cancer cells in a model of i.p. ovarian carcinomatosis (17).

In the present study, we evaluated the ability of incadronate (INC), an N-BP, to inhibit the growth of disseminated pancreatic cancer *in vivo*. We established an *in vivo* pancreatic cancer model with i.p. carcinomatosis in nude mice. INC administration started from the day of tumor inoculation, and reduced tumor burden and ascites accumulation. Additionally, we evaluated the effect of INC on the inhibition of pancreatic cancer cell proliferation, migration, and invasion *in vitro*.

Materials and methods

Cell culture. SUIT-2, AsPC-1, and BxPC-3 cell lines were derived from a human pancreatic ductal adenocarcinoma (PDAC). They were cultured in a RPMI-1640 medium (Invitrogen, Carlsbad, CA, USA) supplemented with 5% fetal bovine serum (FBS) and 50 U/ml penicillin and 50 μg/ml streptomycin in a humidified atmosphere under 5% CO_2 at 37°C.

In vitro cell proliferation assay. Cell proliferation was measured using an MTT dye reduction method (18). Briefly, human PDAC cell lines were seeded into 96-well plates ($5x10^3$ cells/100 μl) and allowed to attach for 24 h. Cells were treated with various concentrations of INC (Astellas Pharma, Tokyo, Japan) for 48 h in 100 μl culture medium. At the end of drug exposure, 5 μl MTT stock solution (5 mg/ml PBS) was added to each well, and the cells were further incubated for 4 h at 37°C. Then, 100 μl of DMSO was added to dissolve the dark blue crystals. Absorbance was measured with an MPR-A4 microplate reader (Tosoh, Tokyo, Japan) at test and reference wavelengths of 540 and 620 nm, respectively.

Analysis of apoptosis. SUIT-2 cells were cultured in slide chambers to no more than 50-60% confluence and treated with various concentrations of INC, as described in *in vitro* cell proliferation assay. After 48-h treatment, apoptosis was assessed using an *in situ* cell death detection kit (Roche Applied Science, Mannheim, Germany), following the manufacturer's recommendations. Briefly, cells were washed with PBS once, fixed with 4% buffered paraformaldehyde for 1 h, washed again with PBS, and permeabilized on ice with 0.1% Triton X-100 in 0.1% sodium citrate for 2 min. Slides were rinsed twice with PBS and then incubated for 60 min at 37°C with terminal deoxynucleotidyl transferase enzyme in reaction buffer. The slides were rinsed three times with PBS and mounted with PermaFluor (Thermo Fisher Scientific, Waltham, MA, USA). Samples were analyzed by fluorescence microscopy. TUNEL-positive nuclei were detected by a bright color in condensed or ruptured nuclei. The rate of apoptosis was calculated as the ratio of the number of apoptotic cells to the total number of cells (both apoptotic and non-apoptotic cells).

Cell migration and invasion assays. Transwell cell migration and invasion were evaluated using a 24-well chemotaxis chamber with a membrane of 8 μm pore size (BD Biosciences, Franklin Lakes, NJ, USA). For migration and invasion assays, SUIT-2 cells were incubated in serum-free culture medium with the various concentrations of INC for 24 h and transferred to the upper chamber ($2.5x10^5$ cells/500 μl) with the various concentrations of INC and allowed to migrate through control (non-coated) and Matrigel-coated (8.7 mg/ml) membranes for 24 h, respectively. The lower chambers were filled with culture medium containing 5% FBS with the various concentrations of INC. Non-migrated cells were wiped off with a cotton swab, the filter was stained with Diff-Quik stain solution (Siemens, Munch, Germany), and the number of remaining cells was counted under the microscope. To determine the percent of invasion, the mean number of cells invading through the Matrigel-coated insert membrane was divided by the mean number of cells migrating through the control insert membrane and multiplied by 100.

Rho pull-down assay. The Rho pull-down assay was performed using a Rho activation assay kit according to the manufacturer's instructions (Cytoskeleton, Denver, CO, USA). Briefly, cells ($3x10^5$/ml) were cultured under serum-free conditions with or without various agents for 24 h. After incubation, the cells were stimulated with 2.2 μM LPA for 1 min and lysed in Mg^{2+} lysis buffer. Equal volumes of cell lysates were incubated with Rhotekin-RBD beads. Bound Rho proteins were detected by Western blotting using a monoclonal antibody against RhoA. Western blotting of the total amount of Rho in cell lysates was performed for comparison with Rho activity (level of GTP-bound Rho) in the same samples.

In vivo peritoneal dissemination model of pancreatic cancer. Five-week-old male nude mice (BALB-cAJcl-nu/nu, Clea Japan, Tokyo, Japan) were housed in filtered-air laminar-flow cabinets and were manipulated using aseptic procedures. Procedures involving animals and their care were conducted in conformity with the guidelines of the National Kyushu Cancer Center. To prepare the *in vivo* peritoneal dissemination model, SUIT-2 cells were injected i.p. as a cell suspension into nude mice ($1x10^6$ cells in 200 μl PBS per animal). This model using SUIT-2 is not only simple and reproducible, but also has characteristics that resemble those of human pancreatic cancer. The treatment regimens started on the day of tumor inoculation and continued for 4 weeks. INC was delivered using a PBS vehicle and was administered i.p. every day. The daily doses of INC used were as follows: 0, 0.1, 1, 2, and 3 mg/kg/d. At the end of the treatment period, mice were sacrificed. The volume of ascites was measured, and tumor tissue was excised, weighed, fixed in 10% neutral buffered formalin, and embedded in paraffin. Paraffin sections (5 μm) were used for histological analysis. Sections were stained with hematoxylin and eosin, examined, and photographed under a microscope. Blood samples were collected from the left heart ventricle and assayed for serum CA19-9.

Statistical analysis. Results are reported as the average ± SEM. Group comparisons were performed using a one-way analysis

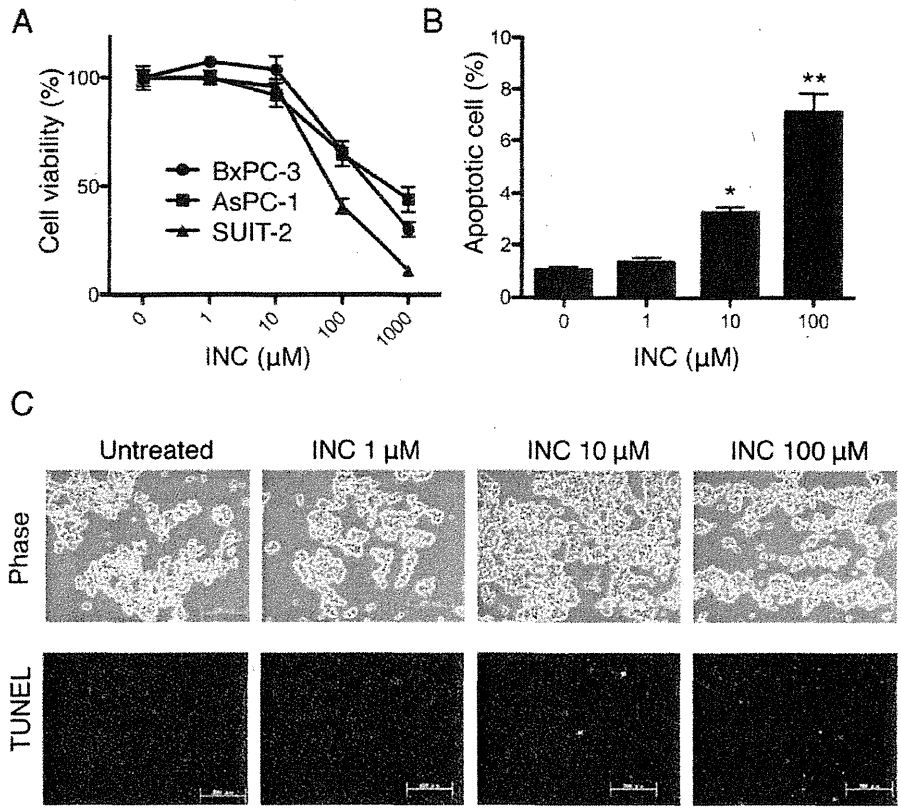

Figure 1. INC induces antiproliferative effects and apoptosis in human PDAC cell lines. (A) BxPC-3, AsPC-1, and SUIT-2 were treated with INC for 48 h. Cell growth inhibition was expressed as a percentage of the absorbance of control cultures measured at 540 nm with a microplate reader. N=6 for each experiment. (B) The rate of apoptosis in SUIT-2 cells treated with INC for 48 h was calculated as the ratio of the number of apoptotic cells to the total number of cells. N=3 for each experiment. *p<0.05, **p<0.01 vs. untreated cells. (C) Representative microscopic photos of SUIT-2 cells treated with INC for 48 h. Phase-contrast microscopy (upper panels) and fluorescent microscopy of TUNEL staining (white) showing apoptotic cells (lower panel). Bar, 200 μm.

of variance (ANOVA) followed by the Tukey-Kramer multiple comparison test. Differences were considered significant at $P<0.05$.

Results

INC induces antiproliferative effects and apoptosis in human PDAC cell lines. The effect of INC on BxPC-3, AsPC-1, and SUIT-2 PDAC cell lines was investigated *in vitro* using the MTT assay. Treatment with INC (1-1000 μM) produced a dose-dependent reduction in cell growth after 48 h of treatment (Fig. 1A) and the IC_{50} was calculated in a range of 50-500 μM. To clarify the mechanisms of INC-induced growth inhibition, we performed a TUNEL assay on SUIT-2 cells, which were the most sensitive to this compound among the three PDAC cell lines tested. Thereafter, we used SUIT-2 cells exclusively in the other experiments. Upon 48-h exposure to INC, the occurrence of apoptosis in 10 and 100 μM INC-treated cells was 3.3 and 7.1% respectively, and was significantly higher than that in untreated cells (1.1%) (Fig. 1B). SUIT-2 cells presented typical apoptotic morphology with cell shrinkage, nuclear condensation and fragmentation, and cellular rupture into debris (Fig. 1C).

Effect of INC on migration and invasion of SUIT-2 in culture. INC was unable to perturb cellular migration toward 5% FBS in chemotaxis chambers at 1 μM (Fig. 2A). At 10 and 100 μM, the inhibition was 49 and 73%, respectively. INC was also potent in its action against the invasion of cells through Matrigel with a 71% inhibition occurring at 10 μM and a 90% inhibition at 100 μM (Fig. 2B). These results are not due to cell cytotoxicity because the degree of cell death after 48-h treatment with INC did not exceed 5 and 10% at 10 and 100 μM INC, respectively. The percent of invasion was 9.6, 10, 5.5, and 3.7% at 0, 1, 10, and 100 μM, respectively (Fig. 2C). Collectively, INC inhibited both migration and invasion of SUIT-2 at a concentration between 10 and 100 μM.

The activation of Rho by LPA is suppressed by INC, and restored by the addition of GGOH in SUIT-2. It is now well established that cell migration is induced by Ras-related GTPases (especially Rho). Soluble factors from serum, such as lysophosphatidic acid (LPA), are thought to activate Rho based on their ability to induce actin stress fibers and focal adhesions in a Rho-dependent manner (19). To evaluate whether LPA induces Rho activity in SUIT-2 cells, we used a pull-down assay with the fusion protein GST- Rhotekin-RBD, which recognizes only Rho-GTP, the active form of Rho. An increase in Rho-GTP was observed in SUIT-2 cells treated for 1 min with LPA (2.2 μM). The inhibitory effect of INC (30 μM) and abrogation by the addition of GGOH (30 μM) suggests INC may inhibit cancer cell migration through Rho geranylgeranylation (Fig. 3).

Effects of INC in a SUIT-2 peritoneal dissemination model. To assess the effect of INC on intraperitoneal dissemination *in vivo*,

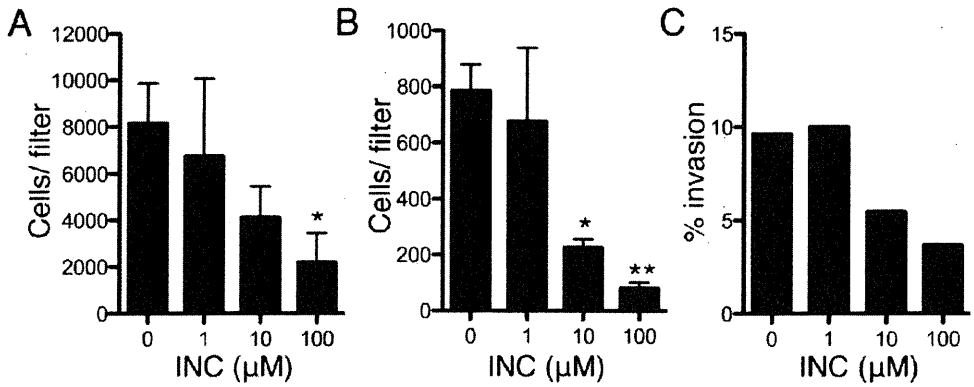

Figure 2. INC inhibits migration and invasion activities of SUIT-2. (A) For migration activity, SUIT-2 ($2.5x10^5$) cells were incubated with the indicated concentration of INC for 24 h and allowed to migrate through non-coated transwell plates for 24 h. (B) For invasion activity, SUIT-2 ($2.5x10^5$) cells were incubated with the indicated concentration of INC for 24 h and allowed to migrate through Matrigel-coated (8.7 mg/ml) transwell plates for 24 h. In either case, after fixing and staining with Diff-Quik stain solution, the number of migrated or invaded cells was counted. Bar, 200 μm. N=3 for each experiment. $^*p<0.05$, $^{**}p<0.01$ vs. untreated cells.

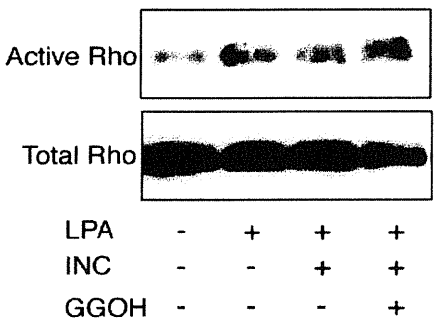

Figure 3. The activation of Rho by LPA is suppressed by INC, and restored by the addition of GGOH in SUIT-2. SUIT-2 cells were cultured under serum-free conditions with or without the various agents indicated for 24 h. After incubation, the cells were stimulated with LPA. The cell lysates were incubated with Rhotekin-RBD beads. Bound Rho proteins were detected by Western blotting using a monoclonal antibody against RhoA (upper panel). Western blotting of the total amount of Rho in cell lysates (lower panel) was performed for comparison with Rho activity (level of GTP-bound Rho) in the same lysates. Blots are representative of three experiments. Relative amounts of active Rho normalized with the amounts of total Rho were determined by densitometric scanning and shown. The concentrations of agents that were used are as follows: LPA 2.2 μM; INC 30 μM; GGOH 30 μM.

we used a pancreatic cancer model with i.p. carcinomatosis in nude mice. We started the administration of INC on the day of cancer cell inoculation. Preliminary experiments revealed that tumor-bearing mice began to exhibit abdominal swelling with ascites ~2.5 weeks after cancer cell inoculation and died from cachexia after the 5th week without any treatment. Therefore, we sacrificed and examined mice 4 weeks after cancer cell inoculation. At the autopsy examination, tumors were found on the surface of the peritoneum, diaphragm, intestines, liver, spleen, pancreas, and kidney, with massive ascites in the control group. The extent of tumor burden varied among the different treatment groups (Fig. 4A). Mean tumor weight in the peritonea of the untreated group was 1.58±0.29 g, and was significantly reduced by ~40% in the group given 1 mg/kg/d (0.63±0.14 g; $p<0.05$), by ~40% in the group given 2 mg/kg/d (0.63±0.15 g; $p<0.05$), and by ~39% in the group given 3 mg/kg/d (0.62±0.13 g; $p<0.05$) (Fig. 4B). Fig. 4C shows the effects of INC treatment on ascites formation. The inhibitory effect of INC on ascites formation was dose-dependent. The mean volume of ascites in the untreated group was 2.91±0.26 ml, and was significantly reduced by ~49% in the group given 1 mg/kg/d (1.42±0.40 ml; $p<0.05$). Strikingly, INC treatment at 2 mg/kg/d and 3 mg/kg/d reduced ascites formation by ~23% (0.67±0.49 ml; $p<0.01$) and by ~21% (0.60±0.28 ml; $p<0.01$), respectively. The concentration of CA19-9, which was expressed from SUIT-2 (20), was examined in the serum collected from the left heart ventricle (Fig. 4D). The effect of INC treatment on the mean concentrations of CA19-9 was dose-dependent, although this did not reach statistical significance. Fig. 4E shows the histological appearance of the tumor nest formed after dissemination in the peritoneum from the untreated group. It shows how the tumor severely invaded into the peritoneum.

Discussion

Pancreatic cancer remains one of the most difficult malignancies to treat. Even patients who are eligible for curative surgical resection gain only moderate benefits. Furthermore, the lack of effective chemotherapeutic and targeted agents highlights the urgent need to better understand pancreatic cancer biology in order to guide the development of novel treatment strategies. During the progression of pancreatic carcinomas, cancer cells released from the surface of the tumor can adhere to and invade tissues and organs in the peritoneal cavity. Consequently, the poor outcome is, at least in part, due to peritoneal dissemination caused by the aggressive migration activity of pancreatic cancer cells (21,22). To undergo peritoneal dissemination, pancreatic cancer cells need to detach from the primary tumor, attach to the cell-extracellular matrix of other tissues, and migrate into the stroma. Once cancer cells migrate into the stroma, angiogenesis occurs from pre-existing capillaries or venulae. Currently available anticancer drugs, even if they are very effective at killing cancer cells, can be used only at limited concentrations because of their toxicity to normal cells. Accordingly, it is worthwhile looking for drugs that inhibit the progression of pancreatic cancer affecting these properties, in addition to cell proliferation.

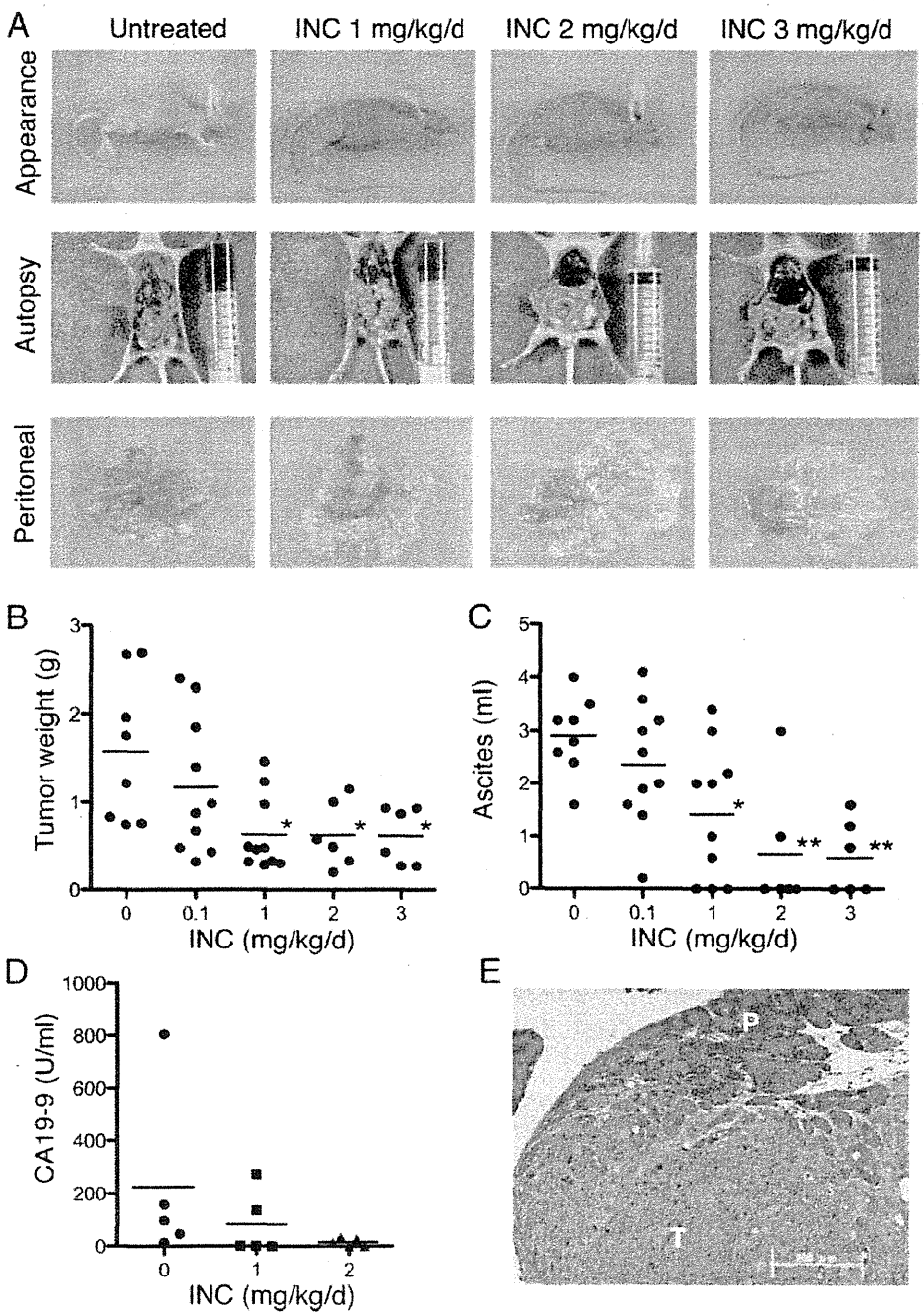

Figure 4. INC inhibits intraperitoneal dissemination in an *in vivo* pancreatic cancer model. (A) A SUIT-2 cell suspension ($1x10^6$/200 μl/ mouse) was injected i.p. into nude mice and treated with the indicated amounts of INC everyday. Mice were sacrificed at 28 days after implantation and ascites, peritoneum, and blood sera were collected. The volumes of ascites (B), the weights of tumors disseminated on the peritoneum (C) and the concentrations of CA19-9 (D) were measured. N=6-10 (B and C); n=5 (D). $^*p<0.05$, $^{**}p<0.01$ vs. untreated mice. (E) Histologic appearance of the tumor nest formed after dissemination in the peritoneum from a SUIT-2-implanted nude mouse. Nude mice were injected i.p. with SUIT-2 cells, sacrificed at 28 days after implantation, and the peritonea were collected. Tissue was fixed, sectioned, and stained with hematoxylin and eosin. T, tumor nest; P, peritoneum, Bar, 200 μm.

Previous reports on the direct effects of N-BPs on cancer cells *in vitro* focused on cell viability and migration/invasion, and the effective concentrations of N-BPs were relatively high (14,16,23,24). According to these reports, the concentrations of alendronate, ibandronate, pamidronate, and zoledronate that induced apoptosis and inhibited invasion of breast, prostate, and ovarian cancer cells were 10-100 μM. The present study also demonstrated that the effective concentrations of INC on the induction of apoptosis and the inhibition of migration/invasion of pancreatic cancer cells were 10-100 μM, whereas the concentration of INC that significantly inhibits osteoclast-like cell formation *in vitro* is 0.01-0.1 μM, which is a clinically used concentration of INC (25). Although it is difficult to treat patients with N-BPs at concentrations of around 10-100 μM because of toxicity, clinical doses may be effective in the treatment of tumors for the following reasons. Tumor-associated macrophages (TAMs) play a pivotal role in tumor growth and metastasis by promoting tumor angiogenesis. Phagocytosis of N-BPs by TAMs

could lead to its depletion by apoptosis and elevate the concentration of N-BPs around the tumor (26).

We evaluated the ability of INC to inhibit the progression of disseminated pancreatic cancer *in vivo*. To accomplish this, we established an *in vivo* peritoneal dissemination model of pancreatic cancer in nude mice. In this model, cancer cells are injected i.p., and, as such, do not reproduce the early events of peritoneal dissemination, i.e. cancer development and detachment from a primary tumor. However, our previous results from a SUIT-2 orthotopic implantation model were nearly identical to those from the i.p. injection model (27), so we decided to use this simple and reproducible model in the present study. Similar to our *in vivo* results from pancreatic cancer cells, the N-BP alendronate, markedly inhibited tumor growth, invasiveness, and ascites formation of human ovarian cancer cells in a model of i.p. ovarian carcinomatosis (17). Such *in vivo* antitumor effects by N-BPs may be derived from the suppression of cancer cell proliferation by apoptosis as well as migration/invasion through the inhibition of molecules in the mevalonate pathway, especially Rho, in the target cancer cells.

This is the first report showing that an N-BP inhibited pancreatic cancer cell invasion to visceral organs *in vivo* and may provide the basis for a new therapy to control the dissemination of pancreatic cancer.

References

1. Kleeff J, Michalski C, Friess H and Buchler MW: Pancreatic cancer: from bench to 5-year survival. Pancreas 33: 111-118, 2006.
2. Ueno H, Kiyosawa K and Kaniwa N: Pharmacogenomics of gemcitabine: can genetic studies lead to tailor-made therapy? Br J Cancer 97: 145-151, 2007.
3. Reni M, Cereda S and Galli L: PEFG (cisplatin, epirubicin, 5-fluorouracil, gemcitabine) for patients with advanced pancreatic cancer: the ghost regimen. Cancer Lett 256: 25-28, 2007.
4. Xu Y, Shen Z, Wiper DW, *et al*: Lysophosphatidic acid as a potential biomarker for ovarian and other gynecologic cancers. JAMA 280: 719-723, 1998.
5. Baker DL, Morrison P, Miller B, *et al*: Plasma lysophosphatidic acid concentration and ovarian cancer. JAMA 287: 3081-3082, 2002.
6. Yamada T, Sato K, Komachi M, *et al*: Lysophosphatidic acid (LPA) in malignant ascites stimulates motility of human pancreatic cancer cells through LPA1. J Biol Chem 279: 6595-6605, 2004.
7. Mills GB and Moolenaar WH: The emerging role of lysophosphatidic acid in cancer. Nat Rev Cancer 3: 582-591, 2003.
8. Horwitz AR and Parsons JT: Cell migration - movin' on. Science 286: 1102-1103, 1999.
9. Chrzanowska-Wodnicka M and Burridge K: Rho-stimulated contractility drives the formation of stress fibers and focal adhesions. J Cell Biol 133: 1403-1415, 1996.
10. Honn KV, Tang DG and Chen YQ: Platelets and cancer metastasis: more than an epiphenomenon. Semin Thromb Hemost 18: 392-415, 1992.
11. Fisher JE, Rogers MJ, Halasy JM, *et al*: Alendronate mechanism of action: geranylgeraniol, an intermediate in the mevalonate pathway, prevents inhibition of osteoclast formation, bone resorption, and kinase activation in vitro. Proc Natl Acad Sci USA 96: 133-138, 1999.
12. Oxford G and Theodorescu D: Ras superfamily monomeric G proteins in carcinoma cell motility. Cancer Lett 189: 117-128, 2003.
13. Jaffe AB and Hall A: Rho GTPases in transformation and metastasis. Adv Cancer Res 84: 57-80, 2002.
14. Virtanen SS, Vaananen HK, Harkonen PL and Lakkakorpi PT: Alendronate inhibits invasion of PC-3 prostate cancer cells by affecting the mevalonate pathway. Cancer Res 62: 2708-2714, 2002.
15. Tassone P, Tagliaferri P, Viscomi C, *et al*: Zoledronic acid induces antiproliferative and apoptotic effects in human pancreatic cancer cells in vitro. Br J Cancer 88: 1971-1978, 2003.
16. Sawada K, Morishige K, Tahara M, *et al*: Alendronate inhibits lysophosphatidic acid-induced migration of human ovarian cancer cells by attenuating the activation of rho. Cancer Res 62: 6015-6020, 2002.
17. Hashimoto K, Morishige K, Sawada K, *et al*: Alendronate inhibits intraperitoneal dissemination in in vivo ovarian cancer model. Cancer Res 65: 540-545, 2005.
18. Green LM, Reade JL and Ware CF: Rapid colorimetric assay for cell viability: application to the quantitation of cytotoxic and growth inhibitory lymphokines. J Immunol Methods 70: 257-268, 1984.
19. Ren XD, Kiosses WB and Schwartz MA: Regulation of the small GTP-binding protein Rho by cell adhesion and the cytoskeleton. EMBO J 18: 578-585, 1999.
20. Iwamura T, Katsuki T and Ide K: Establishment and characterization of a human pancreatic cancer cell line (SUIT-2) producing carcinoembryonic antigen and carbohydrate antigen 19-9. Jpn J Cancer Res 78: 54-62, 1987.
21. Vogel I, Kalthoff H, Henne-Bruns D and Kremer B: Detection and prognostic impact of disseminated tumor cells in pancreatic carcinoma. Pancreatology 2: 79-88, 2002.
22. Su D, Yamaguchi K and Tanaka M: The characteristics of disseminated tumor cells in pancreatic cancer: a black box needs to be explored. Pancreatology 5: 316-324, 2005.
23. Senaratne SG, Pirianov G, Mansi JL, Arnett TR and Colston KW: Bisphosphonates induce apoptosis in human breast cancer cell lines. Br J Cancer 82: 1459-1468, 2000.
24. Hiraga T, Williams PJ, Mundy GR and Yoneda T: The bisphosphonate ibandronate promotes apoptosis in MDA-MB-231 human breast cancer cells in bone metastases. Cancer Res 61: 4418-4424, 2001.
25. Kitagawa Y, Hiraga T, Yura Y and Yoneda T: Suppression by incadronate of invasion and growth of A-375 human melanoma in mandible in nude mice. Oncol Rep 13: 211-216, 2005.
26. Rogers TL and Holen I: Tumour macrophages as potential targets of bisphosphonates. J Transl Med 9: 177, 2011.
27. Iguchi H, Mizumoto K, Shono M, Kono A and Takiguchi S: Pancreatic cancer-derived cultured cells: Genetic alterations and application to an experimental model of pancreatic cancer metastasis. In: Culture of Human Tumor Cells. Pfragner R and Freshney RI (eds.) John Wiley & Sons, Inc., Hoboken, NJ, pp81-96, 2004.

British Journal of Cancer (2012) 107, 1950–1955

www.bjcancer.com

Upregulation of ERCC1 and DPD expressions after oxaliplatin-based first-line chemotherapy for metastatic colorectal cancer

H Baba*[,1], M Watanabe[1], H Okabe[1], Y Miyamoto[1], Y Sakamoto[1], Y Baba[1], M Iwatsuki[1], A Chikamoto[1] and T Beppu[1]

[1]*Department of Gastroenterological Surgery, Graduate School of Medical Science, Kumamoto University, 1-1-1, Honjo, Kumamoto, 860-8556, Japan*

BACKGROUND: The updated randomised phase 2/3 FIRIS study demonstrated the noninferiority of IRIS (irinotecan and S-1) to FOLFIRI (irinotecan, folinic acid, and 5-FU) for metastatic colorectal cancer. Meanwhile, in the subset analysis including patients who previously have undergone oxaliplatin-containing chemotherapy, the IRIS group showed longer survival than the FOLFIRI group. However, the molecular mechanism underlying this result is still unknown.

METHODS: The National Cancer Institute 60 (NCI60) cell line panel data were utilised to build the hypothesis. A total of 45 irinotecan-naive metastatic colorectal cancer patients who had undergone hepatic resection were included for the validation study. The mRNA expressions of *excision repair cross-complementing group 1* (*ERCC1*), *dihydropyrimidine dehydrogenase* (*DPD*), and *topoisomerase-1* (*TOP1*) were evaluated by quantitative RT–PCR. The expressions of ERCC1 and DPD were also evaluated by immunohistochemistry.

RESULTS: Sensitivity to oxaliplatin in 60 cell lines was significantly correlated with that of 5-FU. Resistant cells to oxaliplatin showed significantly higher *ERCC1* and *DPD* expression than sensitive cells. In validation study, *ERCC1* and *DPD* but not *TOP1* expressions in cancer cells were significantly higher in FOLFOX (oxaliplatin, folinic acid, and 5-FU)-treated patients ($N = 24$) than nontreated patients ($N = 21$). The ERCC1 and DPD protein expressions were also significantly higher in FOLFOX-treated patients.

CONCLUSION: The ERCC1 and DPD expression levels at both mRNA and protein levels were significantly higher in patients with oxaliplatin as a first-line chemotherapy than those without oxaliplatin. The IRIS regimens with the *DPD* inhibitory fluoropyrimidine may show superior activity against DPD-high tumours (e.g., tumours treated with oxaliplatin) compared with FOLFIRI.

British Journal of Cancer (2012) **107,** 1950–1955. doi:10.1038/bjc.2012.502 www.bjcancer.com
Published online 20 November 2012

Keywords: DPD; ERCC1; metastatic colorectal cancer; National Cancer Institute; oxaliplatin

The combination of fluorouracil (5-FU) and folinic acid with either oxaliplatin (FOLFOX-4 and FOLFOX-6 regimens) or irinotecan (FOLFIRI and AIO regimens) has been established as the standard first-line chemotherapy for metastatic colorectal cancer (O'Neil and Goldberg, 2008). Second-line therapy for patients whose disease progresses or recurs has been investigated in several clinical studies (Cunningham *et al*, 1998; Rougier *et al*, 1998, 2002; Tournigand *et al*, 2004). Patients who are initially treated with an oxaliplatin-based regimen tend to be offered an irinotecan-based regimen as second-line therapy and vice versa. However, the basic rationale for a sequential treatment strategy has been poorly studied.

An orally administered 5-FU pro-drug, S-1, is approved for the treatment of gastric cancer, colorectal cancer, breast cancer, head and neck cancer, non-small cell lung cancer, pancreatic cancer, and hepato biliary cancer in Japan, and for gastric cancer in Europe. S-1 consists of tegafur, a pro-drug of 5-FU, 5-chloro-2,4-dihydroxypyridine (CDHP), a dihydropyrimidine dehydrogenase (*DPD*) inhibitor maintaining the serum concentration of 5-FU, and potassium oxonate, an inhibitor of orotate phosphoribosyl transferase that reduces gastrointestinal toxicities.

*Correspondence: Dr H Baba; E-mail: hdobaba@kumamoto-u.ac.jp
Received 13 June 2012; revised 8 October 2012; accepted 17 October 2012; published online 20 November 2012

We previously reported the updated results of the randomised phase 2/3 FIRIS study of 426 patients, which reconfirmed the noninferiority of IRIS (irinotecan/S-1) to FOLFIRI using progression-free survival (PFS) as the primary end point (Muro *et al*, 2010; Baba *et al*, 2011). Furthermore, we reported the pre-planned subset analysis that revealed that the median overall survival (OS) of the IRIS group in patients who previously underwent oxaliplatin-containing chemotherapy was significantly longer than that of the FOLFIRI group (adjusted HR = 0.755; 95% CI = 0.580–0.987) (Baba *et al*, 2011). Regarding this intriguing finding, Muro *et al* (2010) have speculated that S-1 might have some salvage effects in patients who previously received FOLFOX, containing oxaliplatin with bolus and infusional 5-FU. However, the mechanism underlying this interaction between the presence or absence of oxaliplatin and therapeutic effects in the FIRIS study remains unclear. The current retrospective study therefore investigated the molecular mechanisms for the superiority of IRIS to FOLFIRI in patients previously treated with oxaliplatin-based chemotherapy.

MATERIALS AND METHODS

NCI60 cell line data

The National Cancer Institute (NCI) database (http://dtp.nih.gov) containing data from 60 NCI60 cell lines was used the

source of cytotoxicity data for oxaliplatin (NSC266046), 5-FU (NSC19893), and DNA copy number. The GI_{50}, which is the concentration required to inhibit growth by 50%, was used as a parameter for cytotoxity. The DNA microarray data for gene expression were downloaded from the Genomics and Bioinformatics group website (http://discover.nci.nih.gov/). Downloaded data were processed and loaded into GeneSpring software, version 7.3 (Agilent Technologies, Santa Clara, CA, USA). Correlations were calculated using Student's *t*-tests with JMP8.0 software (SAS Institute, Tokyo, Japan).

Patient characteristics

Irinotecan-naive metastatic colorectal cancer patients, with Eastern Cooperative Oncology Group performance status (ECOG PS) 0–1, adequate organ function, and resectable liver metastases were enroled in the study. Blocks from resected tumour specimens of liver metastatic lesions were available from 24 patients who preoperatively received the FOLFOX regimen, and 21 with no prior oxaliplatin-containing chemotherapy. All patients underwent hepatic resection for colorectal liver metastasis in the Department of Gastroenterological Surgery, Kumamoto University. The study was carried out in accordance with the Declaration of Helsinki and Good Clinical Practice Guidelines. Written informed consent was obtained from all patients participating in the study. Approval of the protocol was obtained from an Independent Ethics Committee or the Institutional Review Board.

Microdissection

Representative haematoxylin and eosin-stained slides of formalin-fixed, paraffin-embedded (FFPE) blocks were reviewed by a pathologist to estimate tumour load per sample. Section slides of 10-μm thickness were then stained with nuclear fast red (Sigma-Aldrich, St Louis, MO, USA) for manual microdissection. Malignant cells were selected under microscope magnification of $\times 5$ to $\times 10$ and dissected from the slide using a scalpel as described previously (Ceppi *et al*, 2006).

Isolation of RNA and cDNA synthesis

RNA isolation from tumour tissue isolated by manual microdissection and cDNA preparation steps were accomplished as described previously (Kuramochi *et al*, 2006), with a slight modification in the extraction step using RNeasy Mini Elute spin-columns (Qiagen, Chatsworth, GA, USA).

Quantitative real-time PCR

Gene expression levels of *excision repair cross-complementing group 1* (*ERCC1*), *DPD*, and *topoisomerase-1* (*TOP1*) were determined using TaqMan real-time PCR (Life Technologies, Foster City, CA, USA) as described previously (Kuramochi *et al*, 2006). β-Actin was used (*ACTB*) as an endogenous reference gene. All genes were run on all samples in triplicate. The detection of amplified cDNA results in a cycle threshold (Ct) value, which is inversely proportional to the amount of cDNA. Universal Mix RNAs (Stratagene, La Jolla, CA, USA) were used as control calibrators on each plate. The primer sequences for *ERCC1*, *DPD*, and *ACTB* were as previously described (Schneider *et al*, 2005). The Ct was the fractional cycle number at which the fluorescence generated by cleavage of the probe exceeded a fixed level above baseline. The relative amount of tissue target mRNA standardised against the amount of *ACTB* mRNA was expressed as follows: $-\Delta Ct = -(Ct_{(\text{target gene-1})} - Ct_{(\beta\text{-actin})})$. The ratio of the number of target mRNA copies to the number of *ACTB* mRNA copies was then calculated as follows: $2^{-\Delta Ct} \times K$. Here, K is a constant (Livak and Schmittgen, 2001). Contamination with genomic DNA was limited by amplifying nonreverse-transcribed RNA.

Immunohistochemistry

The FFPE tumour tissues were sliced into 4-μm sections. The tissue specimens on the slide were then deparaffinised, and endogenous peroxidase was inactivated. For ERCC1 analysis, the slides were incubated at 4 °C overnight with the primary anti-ERCC1 monoclonal antibody (Clone D-10; Santa Cruz Biotechnology, Inc., Santa Cruz, CA, USA) in a dilution of 1 : 100. For DPD analysis, the slides were incubated at 4 °C overnight with the primary anti-DPD monoclonal antibody (Clone OF-303, Taiho Pharmaceutical Co., Ltd, Tokyo, Japan) in a dilution of 1 : 100. They were then reacted with a reagent containing horseradish peroxidase-labelled polymer-bound anti-mouse IgG (EnVision + system; Dako Japan Inc., Tokyo, Japan). The chromogenic substrate used for detection was DAB (3,3′-diaminobenzidine). Slides were counterstained with haematoxylin.

Immunohistochemical data analysis

The staining intensities of ERCC1 (Kim *et al*, 2009) and DPD (Okabe *et al*, 2000) were evaluated on a scale from 0 to 2+, as described previously with slight modifications. In brief, the positive reaction for both antibodies was scored into three grades, according to the intensity of the staining: 0, 1+, and 2+. The percentages of ERCC1- and DPD-positive cells were also scored into three categories: 0 (0%), 1 (1–49%), and 2 (50–100%). The product of the intensity by percentage scores was used as the final score. The immunostained specimens were independently evaluated by two blinded investigators (HB and HO). There was close agreement (>90%) between the two investigators; in the case of any disagreement, final grading was determined by consensus.

Statistical analysis

Categorical data analysis was conducted using the χ^2 test. The GI_{50} of 5-FU and ERCC1, mRNA level of *ERCC1* and *DPD*, and immunohistochemical score of ERCC1 and DPD were compared using Spearman's correlation coefficient. Either the Student's *t*-test or Wilcoxon test was performed to determine the differences between groups. Results were considered statistically significant at $P<0.05$. All statistical analyses were done with JMP version 8.01 (SAS Institute Inc., Cary, NC, USA).

RESULTS

Data mining in the NCI database

The relationship between the cytotoxic effects of oxaliplatin (NSC266046) and 5-FU (NSC19893) in 60 NCI60 panel cell lines is shown in Figure 1A. The cytotoxic effects of oxaliplatin were significantly correlated with those of 5-FU (Spearman's Rho = 0.55, $P<0.0001$).

For elucidating the underlying mechanism of the correlations between oxaliplatin and 5-FU cytotoxicities, gene expression levels as determined by cDNA microarray analysis were also examined. The NCI60 panel cell lines were arbitrarily classified as oxaliplatin-high-sensitive and oxaliplatin-low-sensitive cell lines according to their respective GI_{50} values. The oxaliplatin-high-sensitive cell lines were those with GI_{50} values within the 15th percentile, whereas the oxaliplatin-low-sensitive cell lines were above the 85th percentile. The remaining cell lines were classified as having intermediate sensitivity.

The Student's *t*-test revealed that the gene expression level of *ERCC1* differed significantly ($P<0.05$) between oxaliplatin-high-sensitive and oxaliplatin-low-sensitive cell lines, as shown in

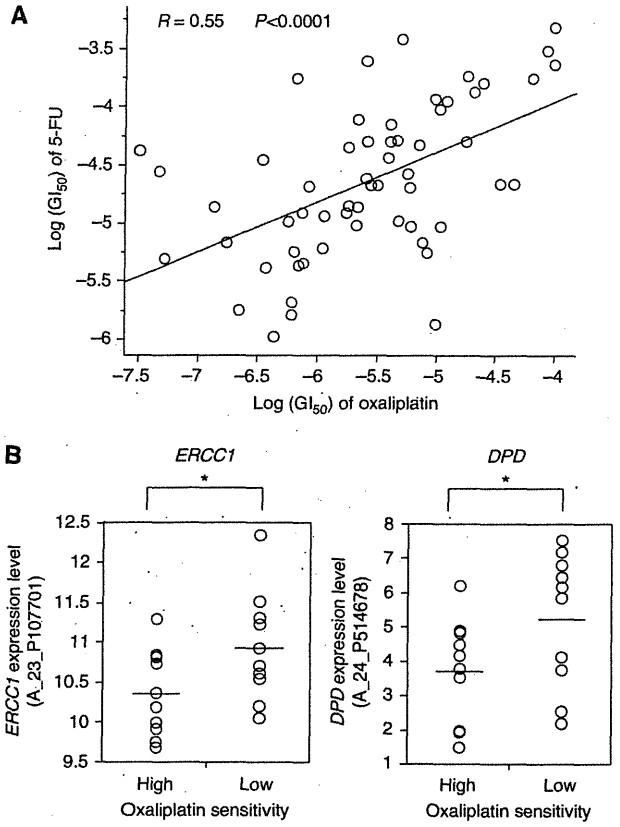

Figure 1 Oxaliplatin-resistant cells showed high *ERCC1* and *DPD* expression in *in silico* analysis. (**A**) Relationship between cytotoxic effects of oxaliplatin (NSC266046) and 5-FU (NSC19893) in 60 NCI60 panel cell lines. (**B**) Comparison of gene expression level, *ERCC1* and *DPD*, or copy number between low sensitive cells and high sensitive cells to oxaliplatin. Data expressed as $\log_2$ (per chip normalised value × 500). $^*P<0.05$.

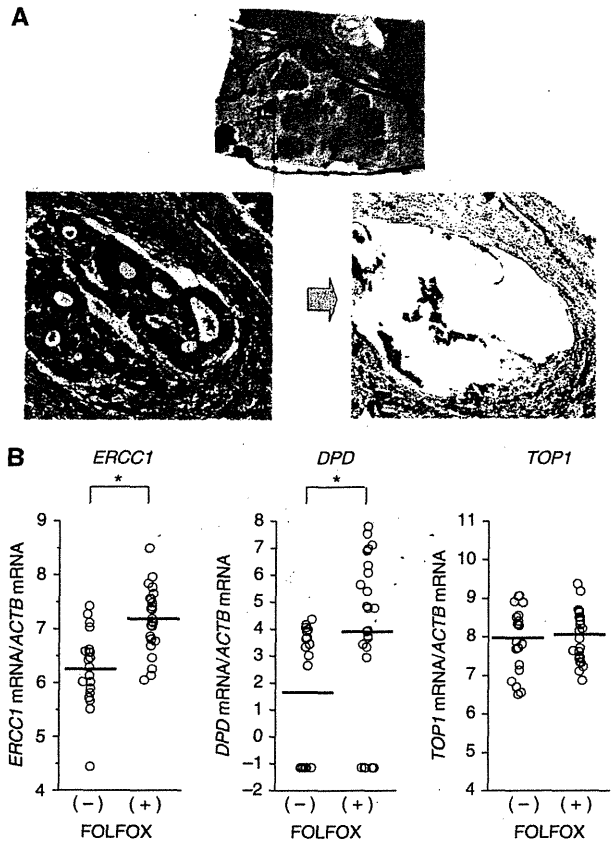

Figure 2 The *ERCC1* and *DPD* mRNAs upregulated in CRC patients with preoperative FOLFOX. (**A**) Typical slide for pathological diagnosis of FFPE tumour specimens (magnification × 2.4). Sections, 5-μm-thick, stained with haematoxylin and eosin before microdissection (magnification × 50). After staining with nuclear fast red, standard manual microdissection was performed (magnification × 50). (**B**) Comparison of gene expression levels of *ERCC1*, *DPD*, and *TOP1* in tumour cells with or without FOLFOX regimen before hepatectomy. $^*P<0.001$ for ERCC1 and $P=0.005$ for DPD, respectively.

Table 1 Patient characteristics

	Oxaliplatin free, $n=21$ (%)	Oxaliplatin treated, $n=24$ (%)	P-value[a]
Gender, no. (%)			0.344
Male	13 (62)	18 (75)	
Female	8 (38)	6 (25)	
Age			0.715
Median, years	62	63	
Range, years	45–75	28–82	
Tumour location (%)			0.974
Proximal colon	3 (14)	3 (13)	
Distal colon	9 (43)	11 (46)	
Rectum	9 (43)	10 (42)	
Differentiation (%)			0.873
Well	10 (48)	12 (50)	
Moderate	11 (52)	12 (50)	
Prior chemotherapy (%)			—
None	19 (90)	—	
5-FU/LV	1 (5)		
S1 + CPT-11 (IRIS)	1 (5)		
mFOLFOX6	—	20 (83)	
mFOLFOX6 + bevacizumab	—	4 (17)	

Abbreviations: 5-FU/LV = fluorouracil/leucovorin; IRIS = irinotecan and S-1; mFOLFOX6 = modified FOLFOX6. [a]The *P*-values for gender were calculated using χ^2 test. The *P*-values for age, tumour location, differentiation, and prior chemotherapy were calculated using the Wilcoxon test.

Figure 1B. Interestingly, the gene expression level of *DPD* also differed significantly ($P<0.05$) between oxaliplatin-high-sensitive and oxaliplatin-low-sensitive cell lines (Figure 1B). Expression levels of *ERCC1* and *DPD* in oxaliplatin-low-sensitive cell lines were 1.5 and 2.9 times higher than those in high-sensitive cell lines, respectively.

Lower sensitivity to oxaliplatin was associated with a parallel increase in *ERCC1* and *DPD* expression. This finding may support that *ERCC1* influences cytotoxicity after oxaliplatin treatment. Based on the findings of recent clinical translational studies (Lentz *et al*, 2005), *ERCC1* was likely a predictive marker for colorectal cancer patients receiving oxaliplatin-containing therapy. Therefore, *ERCC1* was investigated using clinical specimens from patients who had received a first-line chemotherapy with or without oxaliplatin.

Patient characteristics

Table 1 summarises patient characteristics. The median patient age at the time of liver dissection was 62 years (range, 28–82 years). There were no significant differences in clinicopathological factors such as gender, age, tumour location, or differentiation between patients with and without a prior oxaliplatin regimen.

Gene expression level of tumour specimens

The FFPE tumour specimens resected from liver metastasis were subjected to manual microdissection to ensure that only tumour cells were dissected (Figure 2A). As shown in Figure 2B, *ERCC1* and *DPD*, but not *TOP1*, showed statistically significant higher expression in FOLFOX-treated patients ($n=24$) compared with the nontreated group ($n=21$). The mean expression level of *ERCC1* and *DPD* in those receiving the FOLFOX regimen was 1.8 and 4.9 times higher, respectively, than in patients without any prior oxaliplatin-containing chemotherapy (*ERCC1*, $P<0.0001$; *DPD*, $P=0.005$). The expression level of *ERCC1* was significantly correlated with that of *DPD* (Spearman's correlation coefficient = 0.519; $P=0.0003$).

Immunohistochemical results

The RT–PCR analysis revealed higher expression of *ERCC1* and *DPD* in FOLFOX-treated patients than nontreated patients. To confirm the protein expression levels of these genes, immunohistochemical examination was performed. The protein expression of ERCC1 (Figures 3A–C) was found in tumour cells, especially in the nucleus, whereas DPD protein expression was found in tumour cells and stromal cells (Figures 3D–F). For ERCC1, the mean (s.d.) expression was 0.48 (0.68) in patients without FOLFOX and 1.42 (1.41) with FOLFOX (Figure 3G). For DPD, the mean (s.d.) expression was 0.14 (0.36) in patients without FOLFOX and 0.79 (1.02) with FOLFOX (Figure 3G). In accordance with RT–PCR results, immunohistochemical analysis showed that protein expression of both ERCC1 and DPD was significantly higher in FOLFOX-treated patients than nontreated patients ($P=0.015$ and 0.0025, respectively; Figure 3G). Furthermore, a significant correlation between ERCC1 score and DPD score was shown (Spearman's correlation coefficient = 0.65; *P*-value <0.0001).

DISCUSSION

In the present study, gene expression levels of *ERCC1*, which were extracted by the data mining process of NCI60 screening panel data, were significantly higher in recurrent metastatic cancer cells resected from patients who had received the FOLFOX regimen than from patients with no prior oxaliplatin-containing chemotherapy. In addition, the nucleoside catabolic gene *DPD* expression level also showed significant differences between patients with and without oxaliplatin as a first-line regimen. Given that the IRIS regimens with the *DPD* inhibitory fluoropyrimidine may show superior activity against DPD-high tumours compared with FOLFIRI, our

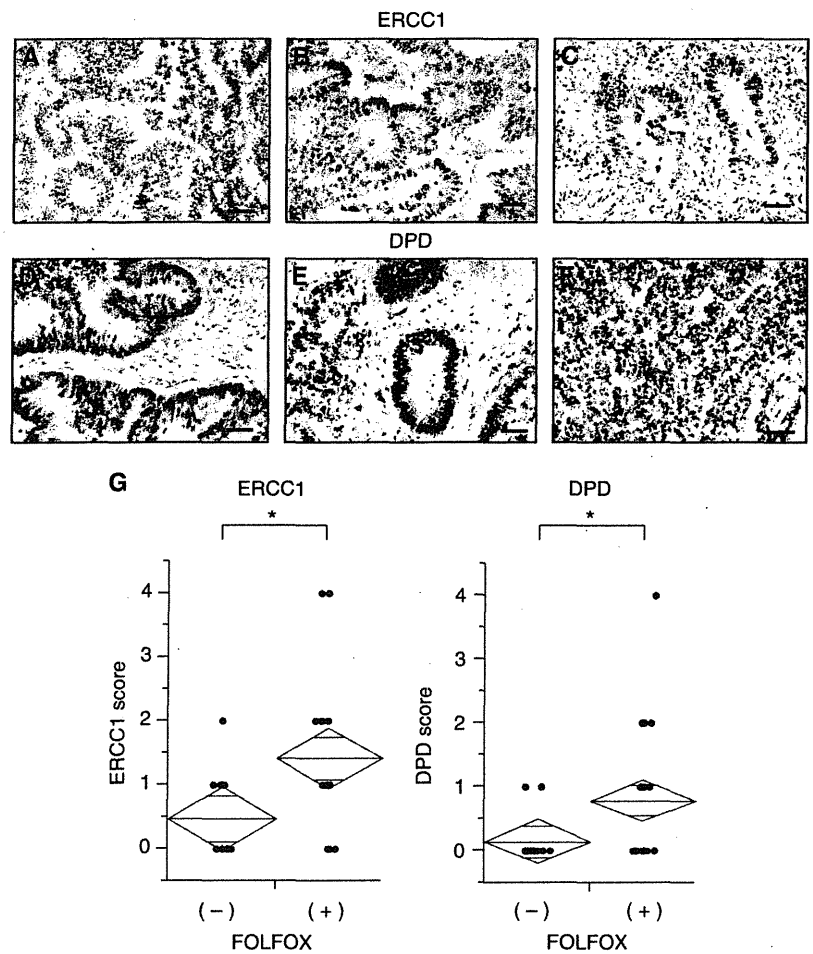

Figure 3 ERCC1 and DPD upregulated in CRC patients with preoperative FOLFOX. Representative pictures of ERCC1 and DPD in CRC patients. Cases of CRC showing weak (**A**), moderate (**B**), and strong (**C**) ERCC1 staining. Cases of CRC showing weak (**D**), moderate (**E**), and strong (**F**) DPD staining; bar = 50 μm. (**G**) The expression scores of ERCC1 and DPD were compared between patients with FOLFOX and patients without FOLFOX using Wilcoxon test. *$P=0.015$ for ERCC1 and $P=0.0025$ for DPD, respectively.

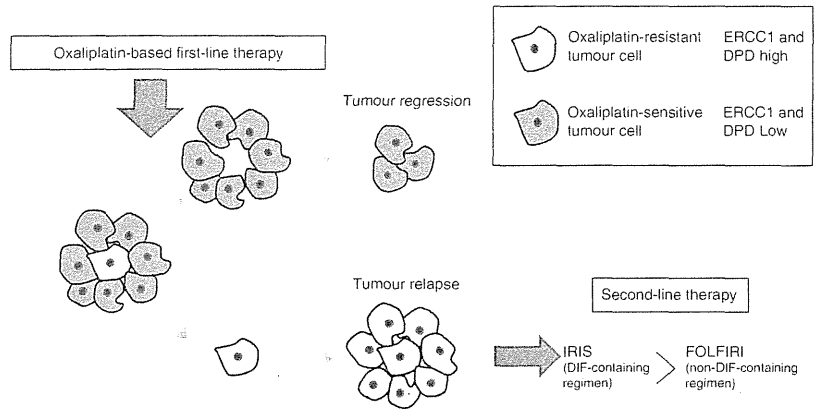

Figure 4 *Hypothesis of molecular mechanism of superiority in IRIS group for prior oxaliplatin-treated patients. This study demonstrated that oxaliplatin-resistant tumour cells showed high ERCC1 and DPD, and thereby seemed to be sensitive to IRIS therapy.*

findings may support the recent clinical result on the superiority of IRIS to FOLFIRI in patients previously treated with oxaliplatin-based chemotherapy.

Colon cancer is known to be a relatively heterogeneous tumour, and is characterised by a heterogenic pool of cells with distinct differentiation patterns. As an example, the *K-ras* mutation was thought to occur during early-stage tumour development; however, a recent study revealed intratumoural heterogeneity of *K-ras* mutations in 35–47% of primary colorectal carcinomas (Giaretti *et al*, 1996; Al-Mulla *et al*, 1998; Losi *et al*, 2005). Baldus *et al* (2010) also reported heterogeneity between primary tumours and lymph-node metastases in 31% (*K-ras*), 4% (*BRAF*), and 13% (*PIK3CA*) of cases. Watanabe *et al* (2011b) found intratumoral heterogeneity of *K-ras* mutations in laser-captured microdissected specimens with respect to discordant *K-ras* status between primary and metastatic colorectal tumours. Such genetic alterations, not only in *K-ras* but also in other genes, could result in intratumoral heterogeneous gene expression (Watanabe *et al*, 2011a). Recently, the concept that cancer might arise from a rare population of cells with stem cell-like properties has received support with regard to several solid tumours, including colorectal cancer (Barker *et al*, 2007; Dalerba *et al*, 2007; O'Brien *et al*, 2007; Ricci-Vitiani *et al*, 2007; Huang *et al*, 2009; Ricci-Vitiani *et al*, 2009; van der Flier *et al*, 2009). Considering the therapeutic implications of cancer stem cells, the failure of current standard therapies to eradicate tumours fully could be explained by assuming that colorectal cancer stem cells are able to survive treatments and achieve only a transitory clinical remission.

Based on our experimental results and knowledge of tumour cell biology, we propose the following hypothesis to explain why the IRIS regimen was superior to the FOLFIRI regimen for colorectal cancer patients who had been treated with oxaliplatin-based regimen. As shown in Figure 4, heterogeneous tumours were exposed to first-line oxaliplatin-containing therapy (mainly the mFOLFOX6 regimen for the FIRIS study, and partly mFOLFOX6 combined with bevacizumab). After the first-line treatment, oxaliplatin-sensitive tumour cells (i.e., *ERCC1* low; illustrated in blue in Figure 4) are killed and a small fraction of relatively oxaliplatin-resistant cells (i.e., *ERCC1* high; illustrated in yellow in Figure 4) survive, which might include cancer stem cells. In NCI60 cell line data, *ERCC1* and *DPD* gene expression is confounding; surviving cells will exhibit high *DPD* gene expression. Consequently, failure of first-line treatment might result in the proliferation of oxaliplatin-resistant tumour cells, which exhibit high levels of *DPD* gene expression. Because the IRIS (S-1/irinotecan) regimen contains S1, the *DPD* inhibitory fluoropyrimidine, it will show superior activity to FOLFIRI (5-FU/LV/irinotecan, non-*DPD* inhibitory fluoropyrimidine) against *DPD*-high tumours. This hypothesis was originally proposed when the updated results of the FIRIS study were reported at the 2011 meeting of the American Society of Clinical Oncology (ASCO) (Baba *et al*, 2011). Molecular mechanisms explaining why *ERCC1* and *DPD* gene expressions seemed to be confounding each other in cancer cells remain unclear. Recently, methylation has been recognised as an epigenetic alteration that leads to gene silencing in human cancer (Estellar, 2003). The role of aberrant methylation of the *DPD* or *ERCC1* promoter as a potential common epigenetic regulatory mechanism in tumour cells remaining after oxaliplatin-based chemotherapy warrants investigation.

A limitation of the present study was the relatively small number of patients included. Nevertheless, the phenomenon identified might be useful in selecting second-line treatments for patients who would benefit the most, and in providing a rationale for selecting therapy. To confirm our hypothesis, the study should be confirmed using an independent cohort of patients. To our knowledge, this is the first report to demonstrate a basic rationale for second-line therapy against the failures of first-line therapy containing oxaliplatin in colorectal cancer patients.

ACKNOWLEDGEMENTS

Our study was supported by an unrestricted technical assistance from Taiho Pharmaceutical Co., Ltd, Japan. We thank Keisuke Miyake, Naomi Yokoyama, and Yuko Taniguchi for their technical support to this report. We also thank Takashi Kobunai for his helpful advice.

REFERENCES

Al-Mulla F, Going JJ, Sowden ET, Winter A, Pickford IR, Birnie GD (1998) Heterogeneity of mutant versus wild-type Ki-ras in primary and metastatic colorectal carcinomas, and association of codon-12 valine with early mortality. *J Pathol* **185**: 130–138

Baba H, Muro K, Yasui H, Shimada Y, Tsuji A (2011) Updated results of the FIRIS study: A phase II/III trial of 5-FU/l-leucovorin/irinotecan (FOLFIRI) versus irinotecan/S-1 (IRIS) as second-line chemotherapy for metastatic colorectal cancer (mCRC). *J Clin Oncol* **29**: 2011 (Suppl; Abstract 3562)

Baldus SE, Schaefer KL, Engers R, Hartleb D, Stoecklein NH, Gabbert HE (2010) Prevalence and heterogeneity of KRAS, BRAF, and PIK3CA mutations in primary colorectal adenocarcinomas and their corresponding metastases. *Clin Cancer Res* **16**: 790–799

Barker N, van Es JH, Kuipers J, Kujala P, van den Born M, Cozijnsen M, Haegebarth A, Korving J, Begthel H, Peters PJ, Clevers H (2007) Identification of stem cells in small intestine and colon by marker gene Lgr5. *Nature* **449**: 1003–1007

Ceppi P, Volante M, Novello S, Rapa I, Danenberg KD, Danenberg PV, Cambieri A, Selvaggi G, Saviozzi S, Calogero R, Papotti M, Scagliotti GV (2006) ERCC1 and RRM1 gene expressions but not EGFR are predictive of shorter survival in advanced non-small-cell lung cancer treated with cisplatin and gemcitabine. *Ann Oncol* **17**: 1818–1825

Cunningham D, Pyrhonen S, James RD, Punt CJ, Hickish TF, Heikkila R, Johannesen TB, Starkhammar H, Topham CA, Awad L, Jacques C, Herait P (1998) Randomised trial of irinotecan plus supportive care versus supportive care alone after fluorouracil failure for patients with metastatic colorectal cancer. *Lancet* **352**: 1413–1418

Dalerba P, Dylla SJ, Park IK, Liu R, Wang X, Cho RW, Hoey T, Gurney A, Huang EH, Simeone DM, Shelton AA, Parmiani G, Castelli C, Clarke MF (2007) Phenotypic characterization of human colorectal cancer stem cells. *Proc Natl Acad Sci USA* **104**: 10158–10163

Estellar M (2003) Relevance of DNA methylation in the management of cancer. *Lancet Oncol* **4**: 351–358

Giaretti W, Monaco R, Pujic N, Rapallo A, Nigro S, Geido E (1996) Intratumor heterogeneity of K-ras2 mutations in colorectal adenocarcinomas: association with degree of DNA aneuploidy. *Am J Pathol* **149**: 237–245

Huang EH, Hynes MJ, Zhang T, Ginestier C, Dontu G, Appelman H, Fields JZ, Wicha MS, Boman BM (2009) Aldehyde dehydrogenase 1 is a marker for normal and malignant human colonic stem cells (SC) and tracks SC overpopulation during colon tumorigenesis. *Cancer Res* **69**: 3382–3389

Kim JS, Kim MA, Kim TM, Lee SH, Kim DW, Im SA, Kim TY, Kim WH, Yang HK, Heo DS, Bang YJ, Lee KU, Choe KJ, Kim NK (2009) Biomarker analysis in stage III-IV (M0) gastric cancer patients who received curative surgery followed by adjuvant 5-fluorouracil and cisplatin chemotherapy: epidermal growth factor receptor (EGFR) associated with favourable survival. *Br J Cancer* **100**: 732–738

Kuramochi H, Hayashi K, Uchida K, Miyakura S, Shimizu D, Vallbohmer D, Park S, Danenberg KD, Takasaki K, Danenberg PV (2006) Vascular endothelial growth factor messenger RNA expression level is preserved in liver metastases compared with corresponding primary colorectal cancer. *Clin Cancer Res* **12**: 29–33

Lentz F, Tran A, Rey E, Pons G, Treluyer JM (2005) Pharmacogenomics of fluorouracil, irinotecan, and oxaliplatin in hepatic metastases of colorectal cancer: clinical implications. *Am J Pharmacogenomics* **5**: 21–33

Livak KJ, Schmittgen TD (2001) Analysis of relative gene expression data using real-timequantitative PCR and the 2(-Delta Delta C(T)) Method. *Methods* **25**: 402–408

Losi L, Baisse B, Bouzourene H, Benhattar J (2005) Evolution of intratumoral genetic heterogeneity during colorectal cancer progression. *Carcinogenesis* **26**: 916–922

Muro K, Boku N, Shimada Y, Tsuji A, Sameshima S, Baba H, Satoh T, Denda T, Ina K, Nishina T, Yamaguchi K, Takiuchi H, Esaki T, Tokunaga S, Kuwano H, Komatsu Y, Watanabe M, Hyodo I, Morita S, Sugihara K (2010) Irinotecan plus S-1 (IRIS) versus fluorouracil and folinic acid plus irinotecan (FOLFIRI) as second-line chemotherapy for metastatic colorectal cancer: a randomised phase 2/3 non-inferiority study (FIRIS study).. *Lancet Oncol* **11**: 853–860

O'Brien CA, Pollett A, Gallinger S, Dick JE (2007) A human colon cancer cell capable of initiating tumour growth in immunodeficient mice. *Nature* **445**: 106–110

O'Neil BH, Goldberg RM (2008) Innovations in chemotherapy for metastatic colorectal cancer: an update of recent clinical trials. *Oncologist* **13**: 1074–1083

Okabe H, Arakawa K, Takechi T, Fukushima M (2000) Expression of recombinant human dihydropyrimidine dehydrogenase and its application to the preparation of anti-DPD antibodies for immunochemical detection. *Gan To Kagaku Ryoho* **27**: 891–898

Ricci-Vitiani L, Fabrizi E, Palio E, De Maria R (2009) Colon cancer stem cells. *J Mol Med (Berl)* **87**: 1097–1104

Ricci-Vitiani L, Lombardi DG, Pilozzi E, Biffoni M, Todaro M, Peschle C, De Maria R (2007) Identification and expansion of human colon-cancer-initiating cells. *Nature* **445**: 111–115

Rougier P, Lepille D, Bennouna J, Marre A, Ducreux M, Mignot L, Hua A, Mery-Mignard D (2002) Antitumour activity of three second-line treatment combinations in patients with metastatic colorectal cancer after optimal 5-FU regimen failure: a randomised, multicentre phase II study. *Ann Oncol* **13**: 1558–1567

Rougier P, Van Cutsem E, Bajetta E, Niederle N, Possinger K, Labianca R, Navarro M, Morant R, Bleiberg H, Wils J, Awad L, Herait P, Jacques C (1998) Randomised trial of irinotecan versus fluorouracil by continuous infusion after fluorouracil failure in patients with metastatic colorectal cancer. *Lancet* **352**: 1407–1412

Schneider S, Uchida K, Brabender J, Baldus SE, Yochim J, Danenberg KD, Salonga D, Chen P, Tsao-Wei D, Groshen S, Hoelscher AH, Schneider PM, Danenberg PV (2005) Downregulation of TS, DPD, ERCC1, GST-Pi, EGFR, and HER2 gene expression after neoadjuvant three-modality treatment in patients with esophageal cancer. *J Am Coll Surg* **200**: 336–344

Tournigand C, Andre T, Achille E, Lledo G, Flesh M, Mery-Mignard D, Quinaux E, Couteau C, Buyse M, Ganem G, Landi B, Colin P, Louvet C, de Gramont A (2004) FOLFIRI followed by FOLFOX6 or the reverse sequence in advanced colorectal cancer: a randomized GERCOR study. *J Clin Oncol* **22**: 229–237

van der Flier LG, Haegebarth A, Stange DE, van de Wetering M, Clevers H (2009) OLFM4 is a robust marker for stem cells in human intestine and marks a subset of colorectal cancer cells. *Gastroenterology* **137**: 15–17

Watanabe T, Kobunai T, Yamamoto Y, Matsuda K, Ishihara S, Nozawa K, Iinuma H, Ikeuchi H, Eshima K (2011a) Differential gene expression signatures between colorectal cancers with and without KRAS mutations: crosstalk between the KRAS pathway and other signalling pathways. *Eur J Cancer* **47**: 1946–1954

Watanabe T, Kobunai T, Yamamoto Y, Matsuda K, Ishihara S, Nozawa K, Iinuma H, Shibuya H, Eshima K (2011b) Heterogeneity of KRAS status may explain the subset of discordant KRAS status between primary and metastatic colorectal cancer. *Dis Colon Rectum* **54**: 1170–1178

British Journal of Cancer (2012) 106, 876–882

www.bjcancer.com

Aberrant activation of the mTOR pathway and anti-tumour effect of everolimus on oesophageal squamous cell carcinoma

K Hirashima[1,2], Y Baba[1,2], M Watanabe[1], R-I Karashima[1], N Sato[1], Y Imamura[1], Y Nagai[1], N Hayashi[1], K-I Iyama[2] and H Baba*[,1]

[1]Department of Gastroenterological Surgery, Graduate School of Medical Sciences, Kumamoto University, 1-1-1 Honjo, Kumamoto 860-8556, Japan; [2]Department of Surgical Pathology, Kumamoto University Hospital, 1-1-1 Honjo, Kumamoto 860-8556, Japan

BACKGROUND: The mammalian target of rapamycin (mTOR) protein is important for cellular growth and homeostasis. The presence and prognostic significance of inappropriate mTOR activation have been reported for several cancers. Mammalian target of rapamycin inhibitors, such as everolimus (RAD001), are in development and show promise as anti-cancer drugs; however, the therapeutic effect of everolimus on oesophageal squamous cell carcinoma (OSCC) remains unknown.

METHODS: Phosphorylation of mTOR (p-mTOR) was evaluated in 167 resected OSCC tumours and 5 OSCC cell lines. The effects of everolimus on the OSCC cell lines TE4 and TE11 *in vitro* and alone or in combination with cisplatin on tumour growth *in vivo* were evaluated.

RESULTS: Mammalian target of rapamycin phosphorylation was detected in 116 tumours (69.5%) and all the 5 OSCC cell lines. Everolimus suppressed p-mTOR downstream pathways, inhibited proliferation and invasion, and induced apoptosis in both TE4 and TE11 cells. In a mouse xenograft model established with TE4 and TE11 cells, everolimus alone or in combination with cisplatin inhibited tumour growth.

CONCLUSION: The mTOR pathway was aberrantly activated in most OSCC tumours. Everolimus had a therapeutic effect both as a single agent and in combination with cisplatin. Everolimus could be a useful anti-cancer drug for patients with OSCC.

British Journal of Cancer (2012) **106,** 876–882. doi:10.1038/bjc.2012.36 www.bjcancer.com
Published online 14 February 2012

Keywords: everolimus; RAD001; mTOR; oesophageal squamous cell carcinoma; proliferation

Oesophageal squamous cell carcinoma (OSCC), the major histological type of oesophageal cancer in East Asian countries, is one of the most aggressive malignant tumours (Enzinger and Mayer, 2003). Despite the development of multimodal therapies, including surgery, chemotherapy, and radiotherapy, the prognosis remains poor even for patients who undergo complete carcinoma resection. The limited improvement in outcomes achieved by conventional therapies urges us to seek innovative strategies, especially those involving molecular targeting, for treating OSCC.

The mammalian target of rapamycin (mTOR) is a 289-kDa serine/threonine kinase involved in cellular growth and homeostasis (Bjornsti and Houghton, 2004; Abraham and Gibbons, 2007; Menon and Manning, 2008; Wouters and Koritzinsky, 2008). Mammalian target of rapamycin is activated by phosphorylation as a part of the phosphatidylinositol-3 kinase/AKT signalling pathway (Mita *et al*, 2003; Chan, 2004; Dancey, 2006) and in turn phosphorylates and activates eukaryotic translation factor 4E (elF4E) and p70 ribosomal S6 kinase (p70S6 kinase), leading to the translation of proteins required for cell cycle progression (Hidalgo and Rowinsky, 2000; Panwalkar *et al*, 2004). The presence and prognostic significance of aberrant mTOR activation have been reported for several types of human carcinomas (Easton and Houghton, 2006; Herberger *et al*, 2007; Hou *et al*, 2007; Hudes, 2009; Hirashima *et al*, 2010). Our group previously showed an association between high phosphorylated mTOR (p-mTOR) expression and poor prognosis in 143 resected OSCC samples (Hirashima *et al*, 2010). Mammalian target of rapamycin has recently been recognised as an important and attractive target for anti-cancer therapy (Boulay *et al*, 2004; Bianco *et al*, 2006; Johnston, 2006; Antonarakis *et al*, 2010; Sparks and Guertin, 2010). Everolimus, an oral mTOR inhibitor, has shown particularly promising results in experimental studies, inhibiting tumour growth and displaying anti-angiogenic effects (Carmeliet and Jain, 2000; Bianco *et al*, 2008; Manegold *et al*, 2008; Lane *et al*, 2009). Combination therapy using everolimus and cisplatin has also been reported to be effective (Beuvink *et al*, 2005; Mabuchi *et al*, 2007; Hou *et al*, 2010; Ma *et al*, 2010). Many clinical trials using everolimus for several types of cancers are currently underway (Yee *et al*, 2006; Fouladi *et al*, 2007; Gridelli *et al*, 2007; Johnson *et al*, 2007; Awada *et al*, 2008; O'Donnell *et al*, 2008; Tabernero *et al*, 2008; Tanaka *et al*, 2008; Yao *et al*, 2008; Wolpin *et al*, 2009). Everolimus has been already approved for the treatment of advanced renal cell carcinoma in patients whose disease has progressed during or after VEGF-targeted therapy (Coppin, 2010). Nonetheless, to our knowledge, no study has examined the therapeutic effect of everolimus on OSCC using *in vitro* and *in vivo* assays.

We therefore conducted this study with three main aims. First, we examined the importance of mTOR activation in OSCC by determining the overall prevalence of p-mTOR expression in OSCC

*Correspondence: Dr H Baba; E-mail: hdobaba@kumamoto-u.ac.jp
Revised 10 January 2012; accepted 11 January 2012; published online 14 February 2012

specimens and cell lines. Second, we evaluated the therapeutic effect of everolimus on OSCC cell lines by both *in vitro* and *in vivo* assays. Third, we specifically assessed the effect of everolimus in combination with cisplatin, which is one of the most frequently used chemotherapeutic drugs, on OSCC cells.

MATERIALS AND METHODS

Reagents and antibodies

Everolimus was provided by Novartis Pharma AG (Basel, Switzerland) and formulated at 2% (w/v) in a microemulsion vehicle. For *in vivo* analysis, everolimus was diluted to the appropriate concentration in double-distilled water just before administration by gavage. For *in vitro* analyses, everolimus was prepared in DMSO just before addition to cell cultures. Antibodies recognising mTOR, phospho-mTOR (Ser^{2448}), p70s6k, phospho-p70s6k (Thr^{389}), 4E-BP1, phospho-4E-BP1 (Thr^{70}), and β-actin were purchased from Cell Signaling Technology (Boston, MA, USA).

Patients

The present study involved 167 consecutive patients who underwent surgical resection of OSCC at the Kumamoto University Hospital from January 1996 to December 2007. None of these patients underwent endoscopic mucosal resection, palliative resection, preoperative chemotherapy, preoperative radiotherapy, or preoperative chemoradiotherapy. This study was approved by the Institute Review Board of the Graduate School of Medical Science, Kumamoto University (Approval number: 236; 2 August 2008).

Immunohistochemistry for p-mTOR

The method of immunohistochemical staining for p-mTOR was described previously (Hirashima *et al*, 2010). Of the 167 tumours, 51 showed no p-mTOR expression, 84 showed weak expression, and 32 showed strong expression. As the aim of the immunohistochemistry in this study was to evaluate the prevalence of p-mTOR expression in OSCC tissues, both weak and strong p-mTOR expression were defined as positive.

Cell culture

Oesophageal squamous cell carcinoma cell lines (TE series) were obtained from the Cell Resource Center for Biomedical Research, Tohoku University. Cell cultures were grown in the recommended medium with 10% foetal bovine serum and incubated in 5% CO_2 at 37 °C.

Western blot analysis

Cultured cells were harvested and lysed in lysis buffer (25 mM Tris-HCl (pH 7.4), 100 mM NaCl, 2 mM EDTA, 1% Triton X-100, leupeptin, 1 mM Na_3VO_4, and 1 mM PMSF) for 30 min. Lysates were centrifuged at 10 000 rpm for 5 min at 4 °C. Each protein sample (10 μg) was mixed with 5 × sample buffer containing 10% β-mercaptoethanol and boiled for 5 min. The total cellular protein extracts were separated by sodium dodecyl sulphate polyacrylamide gel electrophoresis (SDS-PAGE) on 7.5% gels for the examination of mTOR and p-mTOR, and on 12.5% gels for the examination of p70S6K, p-p70S6K, 4E-BP1, p-4E-BP1, and β-actin. The samples were then transferred to PVDF membranes (Bio-Rad, Hercules, CA, USA), which were blocked overnight at 4 °C in 5% skim milk in phosphate-buffered saline (PBS) containing 0.1% Tween 20. The membranes were probed overnight at 4 °C with each primary monoclonal antibody followed by incubation with peroxidase-conjugated anti-rat IgG antibody (1 : 1000) (Sigma, St Louis, MO, USA). The targets were detected using an enhanced chemiluminescence (ECL) reagent (GE Healthcare, Piscataway, NJ, USA).

Cell proliferation analysis

The effect of everolimus on cell proliferation was evaluated using a water-soluble tetrazolium salt (WST-8; (2-(2-methoxy-4-nitrophenyl)-3-(4-nitrophenyl)-5-(2, 4-disulfophenyl)-2H-tetrazolium, monosodium salt) (Dojin Chemicals, Tokyo, Japan). TE4 and TE11 cells were cultured overnight in 96-well plates (3×10^3 cells per well). Cells were then treated for 48 h with everolimus (20 nM) or vehicle (control) and their viabilities were assessed. The number of surviving cells in each sample was determined from its absorbance at 450 nm (A_{450}).

Cell cycle analysis

The cell cycle distribution of TE4 and TE11 cells treated with everolimus (20 nM) or vehicle (control) for 48 h was analysed by flow cytometry using a BD FACSCalibur (BD Bioscience, San Jose, CA, USA) according to previously published methods (Del Bufalo *et al*, 2004; Milella *et al*, 2004).

Apoptosis analysis

TE4 and TE11 cells were treated with everolimus (20 nM) or vehicle (control) for 48 h and then apoptosis was assessed by flow cytometry using Annexin V-FITC (BD Bioscience) and propidium iodide (PI) staining according to previously published methods (Del Bufalo *et al*, 2004; Milella *et al*, 2004).

Invasion analysis

To evaluate the effect of everolimus on cell invasiveness, a Matrigel Invasion Chamber (BD Bioscience) was used according to the manufacturer's protocol. Matrigel-coated chambers containing 8 μm pore-size filters were fitted into 24-well tissue culture plates. Briefly, cells of each type (TE4, 1.0×10^5 cells ml^{-1}; TE11, 5.0×10^5 cells ml^{-1}) were seeded into the Matrigel-coated chambers in RPMI-1640 medium with everolimus (20 nM) or vehicle (control) and incubated at 37 °C in 5% CO_2 for 24 h. The invasive cells on the bottom sides of the filters were stained using Toruijin blue dye, and the numbers of cells in five randomly selected fields at × 200 magnification were counted.

Subcutaneous xenograft model

All the procedures involving animals and their care were approved by the Animal Care and Use Committee of Kumamoto University. These procedures meet the standards required by the United Kingdom Coordinating Committee for Cancer Research (UKCCCR) guidelines (Workman *et al*, 2010). A subcutaneous xenograft model was used to assess the therapeutic effect on OSCC cells of everolimus either as a single agent or in combination with cisplatin, one of the chemotherapeutic drugs most frequently used for OSCC in the clinical setting. Six-week-old nude mice (BALB/c) ($n = 24$) were inoculated subcutaneously in the right or left flank with 5×10^6 TE4 cells and TE11 cells in 200 μl of PBS. Some mice showed insufficient tumour growth and were therefore excluded from the study, leaving a total of 22 mice used for the single *in vivo* experiment. When the tumours reached approximately 50–70 mm^3, the mice were randomised into four treatment groups ($n = 5$–6 mice per group). The first group was treated twice a week with placebo. The second group was treated twice a week with everolimus (5 mg kg^{-1}). The third group was treated every 2 weeks with cisplatin (3 mg kg^{-1}). The fourth group was treated twice a week with everolimus (5 ml kg^{-1}) and every 2 weeks with cisplatin

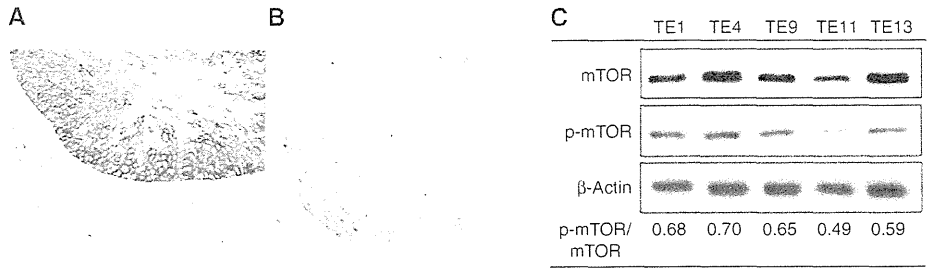

Figure 1 Immunostaining for p-mTOR. (**A**) Oesophageal squamous cell cancer cells positive for p-mTOR (white arrow). (**B**) Oesophageal squamous cell cancer cells negative for p-mTOR. (**C**) Western blot analysis of mTOR, p-mTOR, and β-actin levels in TE1, 4, 9, 11, and 13 cell lines.

($3\,mg\,kg^{-1}$) (Figure 4A). The validity of these everolimus and/or cisplatin protocols has been demonstrated in an ovarian cancer model. Everolimus was administered by oral gavage using an animal-feeding needle. Cisplatin was injected intraperitoneally. Body weight was measured every 3 days. Calliper measurements of the longest perpendicular tumour diameters were made weekly using a digital calliper, and tumour volumes were estimated using the following formula: $V = L \times W \times D \times \pi/6$, where V is the tumour volume, L the length, W the width, and D the depth (Mabuchi *et al*, 2007).

Statistical analysis

For the *in vitro* assays, including the cell proliferation assay, cell cycle ratio assay, apoptosis assay, and invasion assay, statistical analyses were performed using Mann–Whitney's *U*-test for unpaired samples. For the *in vivo* experiment, body weight and tumour volume were compared among placebo-, everolimus-, cisplatin-, and everolimus plus cisplatin-treated mice using the Wilcoxon exact test. Statistical analysis was performed with Stat View-J 5.0 software (Abacus Concepts, Inc., Berkeley, CA, USA). A two-sided significance level of $P<0.05$ was used for all the statistical analyses.

RESULTS

Phosphorylated mTOR expression in OSCC specimens and cell lines

We assessed p-mTOR expression (i.e., mTOR activation) by immunohistochemistry. Of the 167 OSCC specimens, 116 (70%) were positive for p-mTOR expression (Figures 1A and B). The high percentage of p-mTOR-positive tumours supports the crucial role of mTOR activation in the pathogenesis of OSCC.

All five human OSCC cell lines (TE1, 4, 9, 11, and 13) examined in the current study showed p-mTOR expression *in vitro*; the expression level was highest in TE4 cells and lowest in TE11 cells (Figure 1C). Therefore, both TE4 and TE11 cells were used in the following experiments.

Everolimus attenuates phosphorylation of p70S6K and 4E-BP1 *in vitro*

The TE4 and TE11 cells were treated with different concentrations of everolimus (0 (vehicle control), 0.2, 2, and 20 nM) and the levels and phosphorylation of downstream mTOR targets, including p70S6k, p-p70S6k, 4E-BP1, p-4E-BP1, and β-actin (loading control), were evaluated by western blotting. Everolimus inhibited phosphorylation of p70S6k and 4E-BP1 (decreased levels of p-p70S6k and p-4E-BP1) in TE4 cells in a dose-dependent manner (Figure 2). In TE11 cells, 20 nM everolimus was sufficient to block phosphorylation of p70S6k and 4E-BP1 (Figure 2). Therefore, TE4 and TE11 cell lines were treated with 20 nM everolimus in the following assays (e.g., the *in vitro* proliferation, cell cycle, apoptosis, and invasion assays).

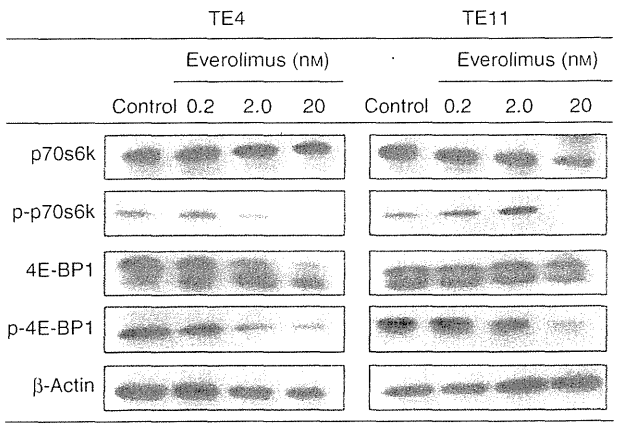

Figure 2 Western blot analysis for p70S6k, p-p70S6k, 4E-BP1 p-4E-BP1, and β-actin protein levels in TE4 and TE11 cells treated with (at indicated concentrations) or without everolimus.

Therapeutic effect of everolimus on OSCC cell lines *in vitro*

Everolimus (20 nM) treatment for 48 h significantly inhibited the proliferation of both TE4 and TE11 cells (Figure 3A). In order to clarify the effect of everolimus on the cell cycle, OSCC cells were treated with everolimus (20 nM) and then subjected to cell cycle analysis by flow cytometry. An accumulation of cells in the G_0/G_1 phase and a reduction in the S-phase fraction were observed in both TE4 and TE11 cells treated with everolimus (20 nM) for 48 h (Figure 3B). Everolimus (20 nM) also significantly increased the proportion of early apoptotic cells (Annexin V-FITC positive, PI negative) compared with that of vehicle-treated cells in both TE4 and TE11 cells treated for 48 h (Figure 3C), indicating that everolimus could induce early apoptosis in these cell lines. Western blot analysis utilising antibodies for Bad and PARP also showed the induction of apoptosis by everolimus (Supplementary Figure 1); everolimus (20 nM) increased the expression of Bad and cleaved PARP protein. Finally, we performed an *in vitro* invasion assay using Matrigel Invasion Chambers and found that everolimus (20 nM) significantly decreased the numbers of invading TE4 and TE11 cells compared with those of vehicle-treated cells (Figure 3D).

Everolimus inhibits tumour growth in a mouse subcutaneous xenograft model

The mean tumour volumes on day 36 in a mouse xenograft model established with TE4 cells were 1314 ± 134, 311 ± 87, 542 ± 161, and

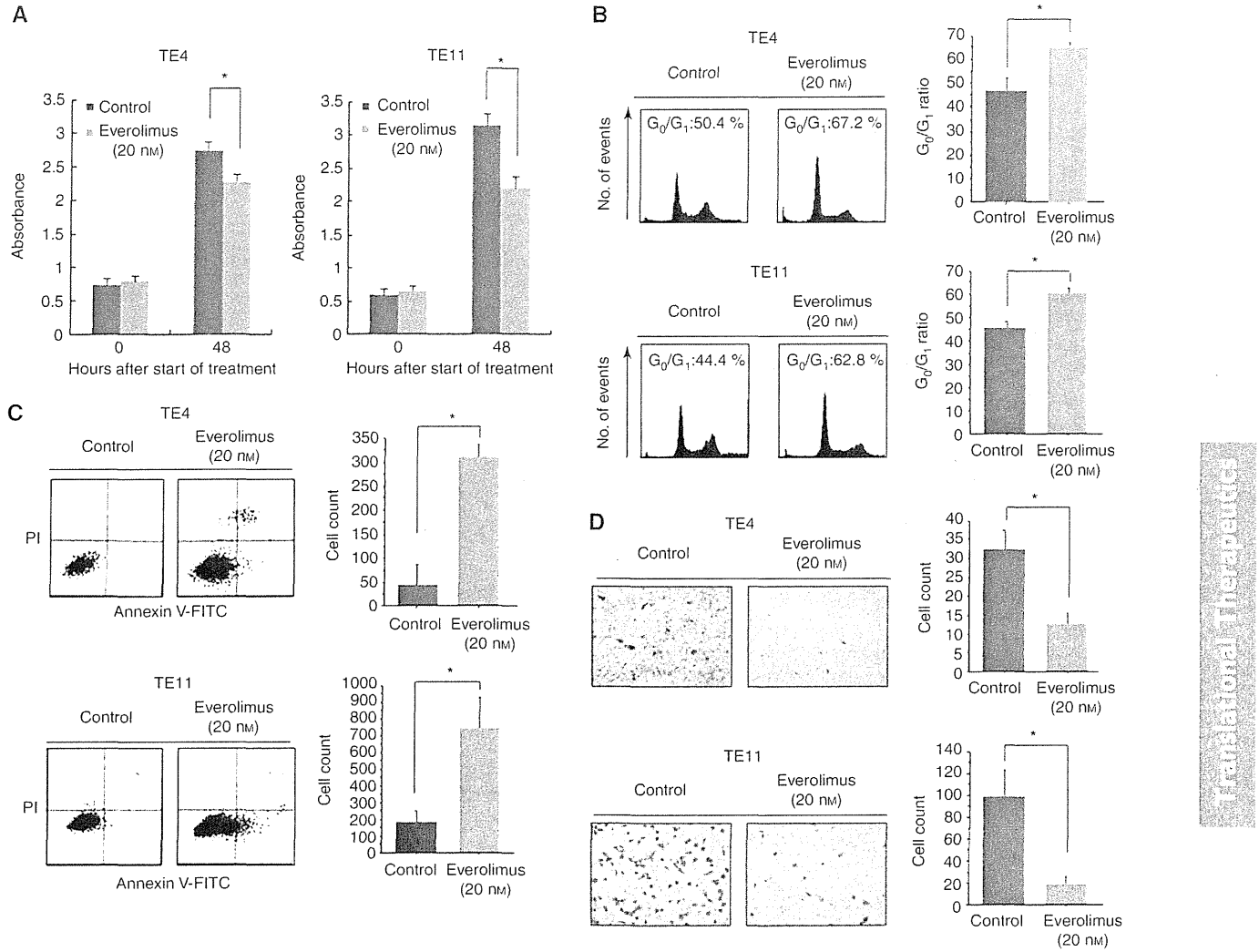

Figure 3 *In vitro* assay for confirming the anti-cancer activity of everolimus. (**A**) *In vitro* proliferation assay. Treatment with everolimus (20 nM) for 48 h decreased the proliferation ratios of both TE4 and TE11 cells compared with those of control vehicle-treated cells. *$P<0.05$. (**B**) *In vitro* cell cycle assay. Treatment with everolimus (20 nM) increased the percentages of TE4 and TE11 cells in G_0/G_1 phase compared with those of control vehicle-treated cells. *$P<0.05$. (**C**) *In vitro* cell apoptosis analysis. Induction of early apoptosis in TE4 and TE11 cells by everolimus is shown (lower right part; Annexin V-FITC-positive, PI-negative). (**D**) *In vitro* invasion assay. Everolimus (20 nM) decreased the numbers of invading TE4 and TE11 cells compared with those of control vehicle-treated cells (× 200 magnification, five fields). *$P<0.05$.

Table 1 Effect of everolimus on tumour development of TE4 cell lines

Treatment	Number of mice	Mean tumour volume (mm^3)	% Effect of tumour reduction
Placebo	6	1314 ± 134	100
Everolimus	5	311 ± 87*,†	23
Cisplatin	5	542 ± 161*	41
Everolimus+cisplatin	6	159 ± 21*,†,‡	12

*Significantly different from the placebo group ($P<0.05$). †Significantly different from the cisplatin group ($P<0.05$). ‡Significantly different from the everolimus group ($P<0.05$).

$159 \pm 21\ mm^3$ in mice treated with placebo, everolimus, cisplatin, and everolimus plus cisplatin, respectively (Table 1, Figure 4B). Treatment with everolimus or cisplatin alone decreased the tumour burdens by 83% and 68%, respectively, compared with that of placebo-treated mice (Figure 4C), indicating that everolimus used as a single agent has marked anti-tumour activity. Moreover, treatment with cisplatin plus everolimus decreased the tumour burden by 92% (Figure 4C), suggesting that the use of everolimus and cisplatin as a combination therapy might be promising. Similar results were obtained for TE11 cells (Supplementary Figure 2).

The weight changes of the mice over the course of the treatments did not differ significantly among the four groups, as shown in Supplementary Figure 3. In addition, we confirmed histologically that there were no differences in the levels of injury to the organs, including liver, kidney, pancreas, lung, intestine, and skin, among these four groups (Supplementary Figure 4). We continued to follow these mice for 2 months. Although all of the mice in the placebo group died within 2 months, no mouse in any of the other three groups died during this period.

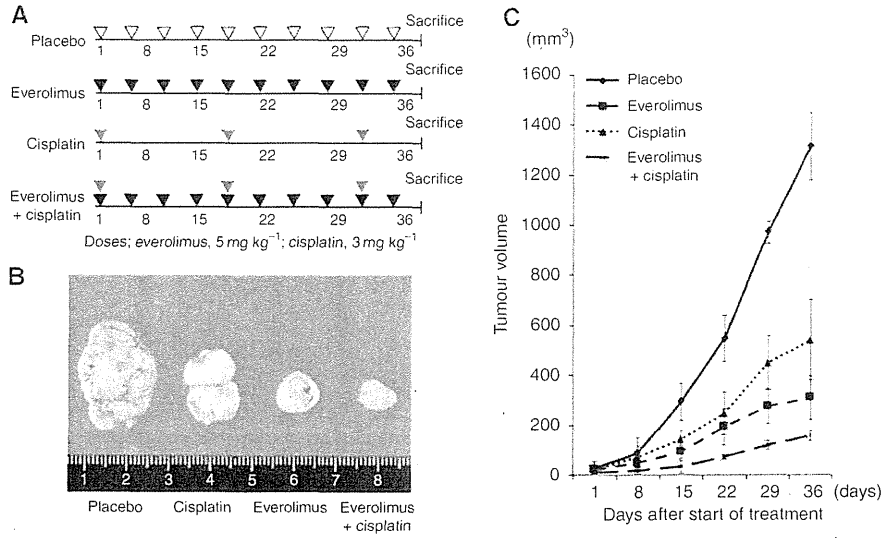

Figure 4 *In vivo* assay for confirming the anti-cancer activity of everolimus utilising a mouse xenograft model established with TE4 cells. (**A**) Treatment schedules for the four treatment groups (placebo, everolimus, cisplatin, and everolimus plus cisplatin). (**B**) Tumour volume in the four treatment groups (placebo, everolimus, cisplatin, and everolimus plus cisplatin) after the 5-week course of treatment. (**C**) Growth of tumour volume in the four treatment groups.

DISCUSSION

Mammalian target of rapamycin is a key regulator of cell growth and proliferation and as such is regarded as a promising target for anti-cancer therapy (Kapoor, 2009; Scott *et al*, 2009). In this study, we made three intriguing findings. First, most OSCC tumours were positive for p-mTOR expression, supporting a role for mTOR activation in the pathogenesis of OSCC. Second, everolimus, an oral mTOR inhibitor, had a therapeutic effect on OSCC cell lines *in vitro*. Third, combination therapy with everolimus and cisplatin showed an additive effect on OSCC cells *in vivo*. Our findings certainly suggest that everolimus could be useful as an anti-cancer drug for patients with OSCC.

Previous studies have shown the importance of mTOR activation in OSCC specimens: Boone *et al*, (2008) detected activated mTOR in 25% of patients with OSCC, a subset of patients that might potentially benefit from mTOR-inhibiting therapy. Yoshioka *et al*, (2008) demonstrated that 48% of OSCC tumours showed high levels of p-mTOR phosphorylation. In the current study utilising 167 OSCC samples, about 70% of the OSCC tumours showed p-mTOR (i.e., mTOR activation). This discrepancy might be due to a difference in the method used to evaluate mTOR phosphorylation or in the cutoff for p-mTOR positivity. Nonetheless, these two previous studies and the current study certainly support the hypotheses that mTOR activation is important in the pathogenesis of OSCC and that mTOR inhibitors might be useful for OSCC treatment.

Everolimus, an orally bioavailable derivative of rapamycin, is a promising drug for cancer therapy. However, to our knowledge, no previous study has utilised *in vitro* and *in vivo* models to evaluate the therapeutic efficacy of everolimus. First, we demonstrated that everolimus suppressed down-stream signalling (i.e., phosphorylation of p70s6 kinase and 4E-BP1) and significantly inhibited cell proliferation and invasion of mTOR-activated OSCC cell lines *in vitro*. Second, we showed that inhibition of mTOR signalling by everolimus induced G_0/G_1 arrest and apoptosis, suggesting that everolimus might inhibit anti-apoptotic or survival signalling in OSCC cell lines. Third, we found that treatment with everolimus significantly inhibited tumour growth *in vivo*. Taken together, these results indicate that everolimus as a single agent could have significant anti-tumour efficacy against OSCC cells.

The effects of everolimus were more prominent in TE11 cells (p-mTOR-low) than in TE4 cells (p-mTOR-high). The malignant characteristics of OSCC cells are likely acquired not only through the mTOR signalling pathway but also through a wide variety of other signalling pathways. Although the activation level of the mTOR pathway was lower in TE11 cells than in TE4 cells, TE11 cells might depend more heavily on the mTOR pathway for their malignant behaviour. On the other hand, although TE4 cells showed a high level of mTOR activation, they might rely more on the other signalling pathways than on the mTOR pathway. In this study, the mTOR pathway was activated in all five cell lines assessed. If we could obtain an OSCC cell line without mTOR activation, those cells might well be resistant to everolimus. Future studies are necessary to confirm our findings as well as to elucidate the biological mechanisms by which the mTOR activation level affects the therapeutic efficacy of everolimus.

Interestingly, we also found an additive effect of everolimus and cisplatin on OSCC cells in an *in vivo* model. A similar effect has been reported for other types of carcinomas. Beuvink *et al*, (2005) reported that everolimus could sensitise cells to cisplatin by inhibiting induction of p21 expression by p53. Ma *et al*, (2010) showed that everolimus exerts an additive-to-synergetic effect on cisplatin-induced growth inhibition in nasopharyngeal carcinoma. Unfortunately, our current experiment could show only an additive effect rather than a synergetic effect. We expect that additional experiments in the future might be able to show a synergetic effect. However, we were at least able to recognise that combining everolimus and cisplatin might be a useful therapeutic strategy. As cisplatin is one of the most important chemotherapeutic drugs for OSCC treatment, our finding may have significant clinical implications.

In conclusion, most OSCC tumours showed mTOR activation, suggesting that mTOR could be a promising target for anti-cancer therapy against OSCC. Everolimus had a therapeutic effect on OSCC cells both *in vitro* and *in vivo*, and combination therapy with everolimus and cisplatin showed an additive effect. Although further experimental studies are necessary to confirm our findings, the current study certainly provides further rationale for future clinical trials of everolimus (in combination with cisplatin) in OSCC patients.